NAVAL POSTGRADUATE SCHOOL
Monterey, California

THESIS

VOLUME REVERBERATION MEASUREMENTS
OF SEDIMENTS
IN THE LABORATORY

by

Joao F. F. Facada

June 1987

Co-Advisor	James V. Sanders
Co-Advisor	Stevens P. Tucker
Co-Advisor	Alan B. Coppens

SECURITY CLASSIFICATION OF THIS PAGE

REPORT DOCUMENTATION PAGE

1a REPORT SECURITY CLASSIFICATION Unclassified	1b RESTRICTIVE MARKINGS
2a SECURITY CLASSIFICATION AUTHORITY	3 DISTRIBUTION/AVAILABILITY OF REPORT Approved for public release; distribution is unlimited
2b DECLASSIFICATION/DOWNGRADING SCHEDULE	
4 PERFORMING ORGANIZATION REPORT NUMBER(S)	5 MONITORING ORGANIZATION REPORT NUMBER(S)
6a NAME OF PERFORMING ORGANIZATION Naval Postgraduate School 6b OFFICE SYMBOL (If applicable) code 68	7a NAME OF MONITORING ORGANIZATION Naval Postgraduate School
6c ADDRESS (City, State, and ZIP Code) Monterey, California 93943-5000	7b ADDRESS (City, State, and ZIP Code) Monterey, California 93943-5000
8a NAME OF FUNDING/SPONSORING ORGANIZATION 8b OFFICE SYMBOL (If applicable)	9 PROCUREMENT INSTRUMENT IDENTIFICATION NUMBER
8c ADDRESS (City, State, and ZIP Code)	10 SOURCE OF FUNDING NUMBERS PROGRAM ELEMENT NO / PROJECT NO / TASK NO / WORK UNIT ACCESSION NO

11 TITLE (Include Security Classification)
VOLUME REVERBERATION MEASUREMENTS OF SEDIMENTS IN THE LABORATORY

12 PERSONAL AUTHOR(S)
Facada, Joao F. F.

13a TYPE OF REPORT	13b TIME COVERED	14 DATE OF REPORT (Year, Month, Day)	15 PAGE COUNT
Master's Thesis	FROM _____ TO _____	1987 June	74

16 SUPPLEMENTARY NOTATION

17 COSATI CODES			18 SUBJECT TERMS (Continue on reverse if necessary and identify by block number)
FIELD	GROUP	SUB-GROUP	volume reverberation, waveform envelope, scattering coefficient, decay constant, sediment

19 ABSTRACT (Continue on reverse if necessary and identify by block number)

The acoustic volume reverberation in sediments of different grain sizes was determined in the laboratory. Three sediments, *fine sand*, *aquarium sand* and *aggregate*, ranging in average grain size from 0.3 mm to 5.3 mm, were selected. An additional material, *glass beads*, with an average particle size of 1.7 mm, was also studied to investigate the influence of inhomogeneities in particle composition.

In the experiment ten sets of 50 scattered pulses of pulse duration 88 μs and 180 kHz carrier frequency were averaged, and the envelope of the decaying tail was fitted with a logarithmic curve. The decay constants for the various sediments showed a variation with the grain size expressed by $a = 10.3 - \eta/0.0035$ where a is the grain diameter in mm and η the decay constant in Np/μs. The value of a can be

20 DISTRIBUTION/AVAILABILITY OF ABSTRACT	21 ABSTRACT SECURITY CLASSIFICATION	
☐ UNCLASSIFIED/UNLIMITED ☐ SAME AS RPT ☐ DTIC USERS	unclassified	
22a NAME OF RESPONSIBLE INDIVIDUAL Stevens P. Tucker	22b TELEPHONE (Include Area Code) (408) 646-3269	22c OFFICE SYMBOL code 68Tx

DD FORM 1473, 84 MAR 83 APR edition may be used until exhausted
All other editions are obsolete

SECURITY CLASSIFICATION OF THIS PAGE

estimated within ± 2.8 mm for a decay constant of 2.5×10^{-2} Np/μs. This relation is limited to the specific equipment used in the experiment and to the frequency of 180 kHz.

Approved for public release; distribution is unlimited.

Volume Reverberation Measurements of Sediments in the Laboratory

by

Joao F. F. Facada
Lieutenant, Portuguese Navy
B.S., Portuguese Navy Academy, 1977

Submitted in partial fulfillment of the
requirements for the degree of

MASTER OF SCIENCE IN HYDROGRAPHIC SCIENCES

from the

NAVAL POSTGRADUATE SCHOOL
June 87

ABSTRACT

The acoustic volume reverberation in sediments of different grain sizes was determined in the laboratory. Three sediments, *fine sand*, *aquarium sand* and *aggregate*, ranging in average grain size from 0.3 mm to 5.3 mm, were selected. An additional material, *glass beads*, with an average particle size of 1.7 mm, was also studied to investigate the influence of inhomogeneities in particle composition.

In the experiment ten sets of 50 scattered pulses of pulse duration 88 μs and 180 kHz carrier frequency were averaged, and the envelope of the decaying tail was fitted with a logarithmic curve. The decay constants for the various sediments showed a variation with the grain size expressed by $a = 10.3 - \eta/0.0035$ where a is the grain diameter in mm and η the decay constant in Np/μs. The value of a can be estimated within ± 2.8 mm for a decay constant of 2.5×10^{-2} Np/μs. This relation is limited to the specific equipment used in the experiment and to the frequency of 180 kHz.

TABLE OF CONTENTS

LIST OF TABLES

LIST OF FIGURES

ACKNOWLEDGEMENTS

I wish to express my appreciation to Lieutenant Commander David Gardner who gave me enthusiasm to join this project, to Lieutenant Chang (Republic of China) for his fellowship in teaching me the experimental procedures, to Lieutenant F. Rossman and R. Koehler for helping me in giving a better presentation to my thesis and to Professors James Sanders, Alan Coppens and Stevens Tucker for their technical advice and direction. I want also to thank my parents for their encouragement and prays, my wife Ana and my son Joao Diogo for their support and company in the moments of higher stress and most of all I thank the LORD.

This is the final step of two years of a beautiful experience lived in a friendly country where so many friends were met and whose friendship I will never forget. "Though the mountains divide and the oceans are wide" this school will be always very present to me.

I'll miss you America !!

I. INTRODUCTION

The first use of sound to detect underwater objects by echo-ranging was in World War I, but it was not until World War II that sonar development became significant. Detection and ranging are the main functions of sonar systems, which include the fathometer, a widely used and very important application. The fathometer measures the round-trip travel time of short sound pulses between a transmitter located at the water's surface and the bottom. If the sound speed in the water is known, depth measurements are possible and the safety of navigation in near-shore areas is improved.

The fundamental principle is simple but the process involves some complexity due to the variation in sound speed and attenuation in the water. These processes are inherent to the water, but when a target or the bottom is present, reflection, absorption and incoherent scattering at the interface between the target or bottom must be considered.

This is the situation present in a hydrographic survey operation: A transducer in the water sends sound pulses to the bottom which are reflected back. Along the sound path transmission losses due to spreading, absorption and scattering occur. Changes in temperature, salinity and pressure along the path of a sound ray cause refraction, which is not a very important problem in hydrography, because the transmitter points downward. Upon reaching the bottom, sound is both reflected and transmitted into the bottom so that its amplitude is decreased. Some of the sound transmitted into the bottom is scattered backward where it combines with the reflected pulse, distorting the initial pulse shape. This pulse distortion is the subject of this paper.

In hydrography it is the front edge of the received pulse which is normally of interest, since it gives the distance to the bottom. In addition, however, more information may be obtained from the same received pulse. In fact, the tail of the received signal can give information about the nature of the bottom. There is thus the possibility to remotely classify the bottom type, an operation essential to the preparation of nautical charts.

The intent of this project is to verify a laboratory technique previously studied and established by Diaz (1986) and Chang (1986), in which the trailing edge of the

reflected pulse is characterized in terms of a straight line fitted to the envelope by a least square method. In this study the same experimental procedures are applied to natural sediments and artificial materials to test the theory relating the type of bottom sediment to the received echo level.

II. THEORETICAL CONSIDERATIONS

A. DEFINITION OF REVERBERATION

In any echo-ranging or listening device the desired signal is always received in the midst of a certain amount of extraneous noise (National Defense Research Commitee,1969). Particularly in underwater acoustics, this noise can arise from different sources such as breaking waves, snapping shrimp, surf and shipping, which combine to produce broadband ambient noise (Kinsler, Frey, Coppens and Sanders, 1983).

However if dealing with an active system like the sounding equipment used in hydrography, another type of interference arises, which is directly due to the transmission of the pulses into the water. This component is called reverberation and results from the existence of particles or discontinuities in the path of the pulse that act as small scattering centers, reradiating the acoustic energy and returning a weak echo to the transducer. The combination of all these small echoes makes the reverberation. Like ambient noise, reverberation is usually undesired, because it masks the reflected signal.

1. Surface, Bottom and Volume Reverberation

When small scatterers or discontinuities are observed along a reflecting surface, like the water-air interface, surface reverberation occurs. It is important when a reflecting surface has a certain roughness compared to the wavelength of the sound. When the reflection is produced at the bottom surface, and if this bottom surface shows some irregularities or small objects, then bottom reverberation is produced. But, if the reverberation is due to scatterers existing in the body of the propagation medium, i.e. the water column, then we have volume reverberation. In this project the volume reverberation produced in the sediment is of interest because, as it was pointed out before, the amount of volume reverberation observed can give an indication of the type of sediment present. This suggests the possibility of rapidly determining the types of bottom sediments present during hydrographic soundings.

2. Reverberation Level

If an active system with an intensity I_0 at the transmitter is considered, with a target at range r, the intensity level, IL(r), of the signal reaching the target is

$$IL(r) = 10 \log [I(r)/I_{ref}] \text{ dB} \tag{2.1}$$

where

$$I(r) = I_0/r^2 \tag{2.2}$$

for transmission loss by spherical spreading.
After being scattered by a volume, dV, the intensity level depends on the ability of the target to reflect the incident energy. This ability is expressed by S_V, the scattering strength.

$$S_V = 10 \log s_V \tag{2.3}$$

where s_V is the scattering coefficient per unit volume

$$s_V = \sigma/4\pi \tag{2.4}$$

and σ is the backscattering cross section of the unit volume. Thus, the scattered intensity, $I_s(r)$ at 1 m from the target is

$$I_s(1) = (I_0/r^2)s_V V \tag{2.5}$$

where V is the volume occupied by scatterers that contribute to the reverberation received at the receiver at time t. One essential step in obtaining the reverberation level (RL) is to compute the scattering volume which is a function of the transmitting pulse length (τ), and the directivity of the transducer (here assumed monostatic). The geometry occurring in hydrographic surveying is shown in Figure 2.1.

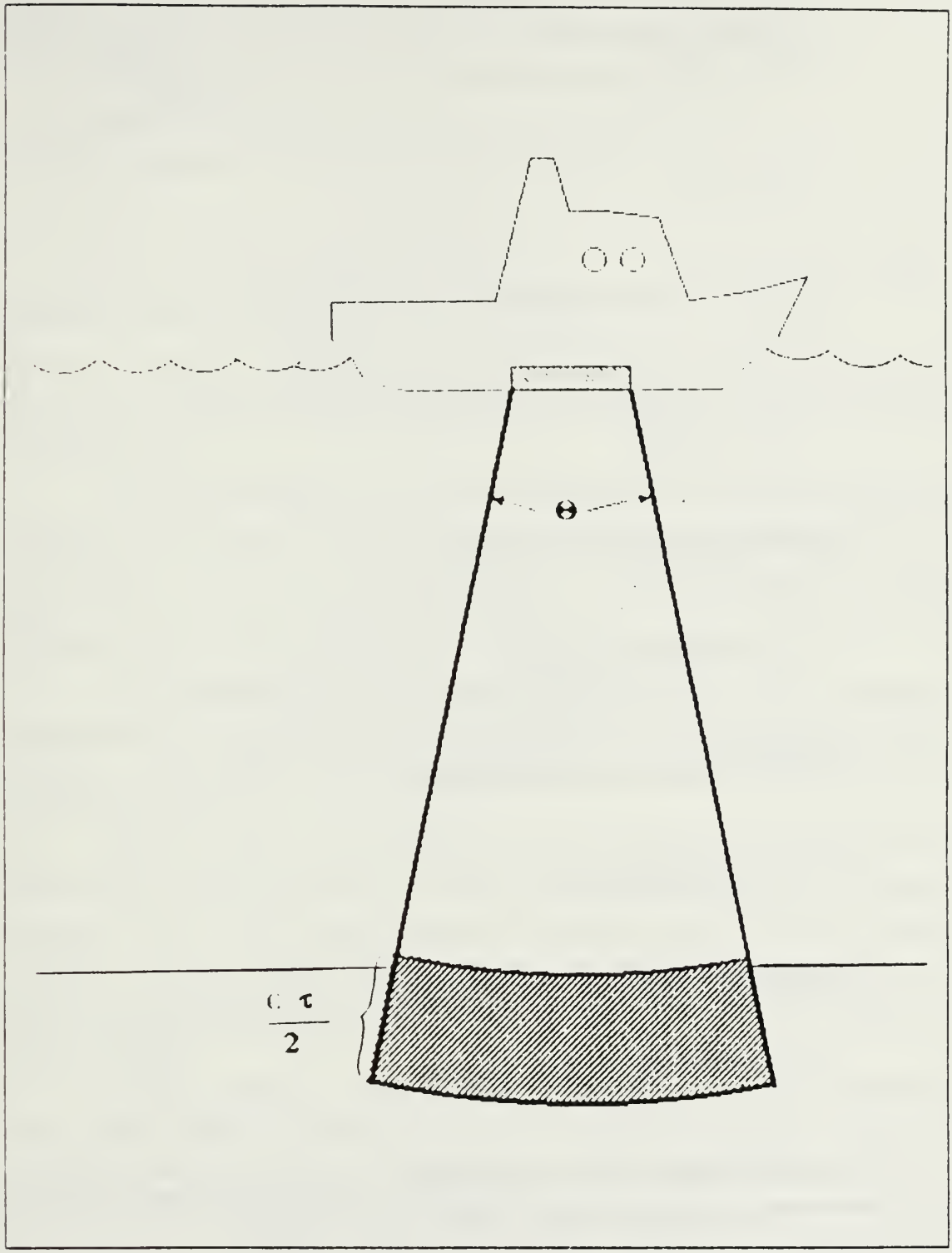

Figure 2.1 Echo sounding geometry and elementary portion of volume reverberation contribution.

The thickness of the reverberating volume must be such that all the scatterers in it contribute reverberation at the same time at the receiver, (Kinsler, Frey, Coppens and Sanders, 1983) and that depends directly on the pulse length or

$$L = c\tau/2 \tag{2.6}$$

where τ is the pulse duration. For a geometric cross section of the beam pattern, A, we have

$$V = Ac(\tau/2) \tag{2.7}$$

Substituting this into Equation 2.5 gives

$$I_s(1) = (I_0/r^2)s_v Ac(\tau/2) \tag{2.8}$$

and the intensity at the receiver becomes

$$I_s = (I_0/r^4)s_v Ac(\tau/2) \tag{2.9}$$

The volume reverberation level in the form of a sonar equation is

$$RL = SL - 40 \log r + S_v + 10 \log V \tag{2.10}$$

Urick (1983) suggests that in reverberation backgrounds it is easy to find the echo-to-reverberation ratio for a target of known target strength:

$$EL = SL - 2TL + TS \tag{2.11}$$

where

EL = echo level

SL = source level

TS = target strength

Subtracting Equation 2.10 from Equation 2.11 we obtain

$$EL - RL = TS - (S_v + 10 \log V) \qquad (2.12)$$

but (S_v + 10 log V) is the reverberation target strength, and the echo-to-reverberation ratio is only the difference of two strengths, one for the reflected echo and the other for the scattered one.

How can this suggestion be applied to our project ? In it we are interested in finding the RLs produced by different materials. Considering the reflection only at the fluid-sediment interface (no incoherent surface or volume scattering), the reflected signal will have the same shape, no matter which material is below that interface, being reduced in amplitude only by the reflection coefficient of the sediment.

If the incoherent scattering produced by the sediment particles is added the received scattered signals will differ in shape, (mainly in the trailing edges) for different sediments. These differences are due to the incoherent scattering represented in the sonar equation by RL.

There is no way to measure directly the pure (coherent) pulse reflected at the water-sediment interface because the reflected signal is "contaminated" by incoherent scattering, but it can be approximated by the pulse reflected from the water-air interface. The only difference between these is the voltage amplitude because the specific acoustic impedances are different, but this can be corrected by normalizing the received voltages.

In Chang (1986) this pure, reflected signal was obtained using a transducer lying on the bottom and transmitting upward to the water-air interface. The signal received is then purely reflected, assuming that no surface reverberation is produced at the interface or that its magnitude is negligible compared to the volume reverberation produced in the sediment. This assumption also applies to the water-sediment interface, which must be perfectly level and smooth.

By using the same transmitting conditions, but with the transducer located at the water-air interface and transmitting downward to the bottom, a different signal is received back in the transducer; this represents the volume reverberation.

Geometrically this procedure can be illustrated with the pictures of the two distinct waveform envelopes. Besides the difference in amplitude, the most noticeable feature is that the received waveform shows a slower decaying of its tail, where reverberation is geometrically expressed. Mathematically, the decaying tail can be represented by

$$V_w(t) = V_0 e^{-\alpha t} \tag{2.13}$$

for the water-air interface and

$$V_s(t) = V_0 e^{-\eta t} \tag{2.14}$$

for the water-sediment interface, where V_0 is normalized to the same value in each case (Chang,1986). The difference between these two expressions gives a measure of the amount of volume reverberation coming from that particular sediment.

$$\Delta V(t) = V_0(e^{-\eta t} - e^{-\alpha t}) \tag{2.15}$$

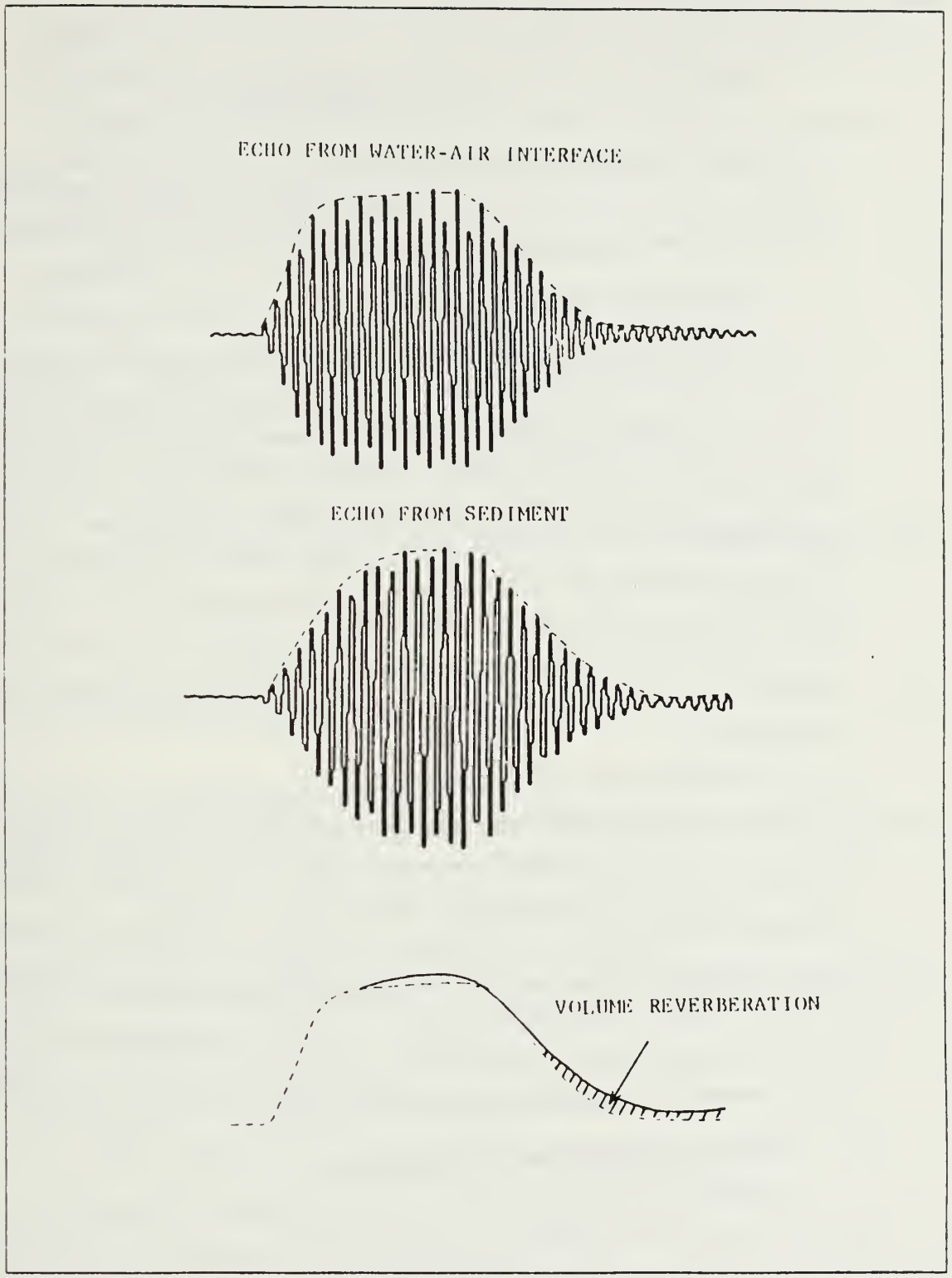

Figure 2.2 Geometric interpretation of volume reverberation.

III. BACKGROUND

Many research projects have been devoted to the study of reverberation in the ocean. However, most have been concerned with scattering produced in the water column and only a few with volume reverberation in marine sediments.

A. LITERATURE REVIEW

Urick (1953) studied backscattering from the bottom as a function of pulse length, frequency and grazing angle at several locations in a harbor using a tiltable transducer mounted on a barge. The results were expressed in terms of scattering strength per unit area of bottom. Mackenzie (1961) made bottom-reverberation measurements using two low frequencies and different pulse lengths as well as different grazing angles. He analysed the data to obtain scattering coefficient for the bottom. McKinney and Anderson (1963) made the same measurements but for three different types of sediment: mud, sand and gravel. They concluded that the bottom sediment is a major factor in the backscattering of sound and that the knowledge of particle size distribution of the sediment is useful in estimating the reverberation level. No model was formulated.

Recent relevant work (Dodds [1982,1984], Breslau [1967] and Meng [1982]) deals with the problem of using backscattering measurements to remotely classify bottom types. Dodds used a broadband acoustic source (1-10 Khz) directed vertically to the sea floor and obtains sonograms from which volume scattering and surface roughness parameters are obtained. Meng (1982) discussed the classification of seabed sediments, based on the echo envelope of normally reflected high-frequency sound pulses. This is apparently similar to the present work. It would be interesting to investigate his procedure, processing and achievements. However this paper was published in Chinese, and only a short abstract is available in English.

B. VOLUME REVERBERATION MODELS

The backscattering of sound from the ocean bottom has been studied for many years, but apparently only Morse and Ingard (1968) and Urick (1983) have developed theoretical models appliable to the present study.

These models have, however, a restricted application since they make several assumptions that are not satisfied in the present case, where the wavelength is 8 mm and the average diameter of the scatterers is between 0.3 and 5.3 mm.

Morse and Ingard's assumptions and their relevance to the present study are:

1) Scattering objects are small compared with the wavelength.
(satisfied here only for the fine sand).

2) Dimensions of the scattering region are much larger than the wavelength.
(Assumption satisfied for all four sediments).

3) The scatterers are all spheres. (Not too bad an assumption for all four sediments).

4) The scatterers are sparsely packed and no multiple scattering is considered. (Very poor assumption for all sediments).

For monostatic sonars Morse and Ingard give the volume scattering coefficient per unit volume as

$$s_v = N (2\pi)^{1/2} k^6 a^8 (\gamma_\kappa - \gamma_\rho)^2 \qquad (3.1)$$

where "a" is the radius of the scatterers, N the number of scatterers per unit volume and k is the wave number,

$\gamma_\kappa = (\kappa_n - \kappa_o)/\kappa_o$

where κ_n is the compressibility of the scatterer, κ_o the compressibility of the fluid and

$\gamma_\rho = (3\rho_n - 3\rho_0) / (2\rho_n - \rho_o)$

where ρ_n is the scatterer density and ρ_o the fluid density.

The scattering coefficient per unit volume as given by Urick (1983) is

$$s_v = N \sigma \qquad (3.2)$$

where σ, the backscattering cross section, is given by

$$\sigma = 2.8\,(\pi\, a^2)(k\, a)^4 \qquad (3.3)$$

where "a" is the scatterer dimension. This model is good for a single sphere (no multiple scattering) and for values of $Ka << 1$.

C. DERIVED MODEL

The present project is an extension of the recent work developed by Diaz (1986) and Chang (1986). Chang measured volume reverberation on *aggregate* and *fine sand* to compute the corresponding volume-scattering coefficients. Applying Morse and Ingards (1968) and Urick's (1983) models Chang did not get satisfactory results, verifying that these models are not appropriate for ocean sediments. A simple model was then set up:

The envelope of the electrical pulse shape can be described by a square wave of pulse duration τ

$$I(t) = I_o[H(t) - H(t-\tau)] \qquad (3.4)$$

where

$I(t)$ = intensity at time t after the beginning of the pulse

I_o = constant intensity amplitude

τ = pulse length

$H(t)$ = unit step function shown in Figure 3.1 a)

$$H(t) = \begin{cases} 0 & t<0 \\ 1 & t>0 \end{cases}$$

$H(t-\tau)$ is then: (Figure 3.1 b))

$$H(t-\tau) = \begin{cases} 0 & t-\tau<0 \\ 1 & t-\tau>0 \end{cases}$$

The transmitted pulse is not exactly square due to damping of the transducer, but it is tranformed into an acoustic pulse with an exponential rise, a flattened top and an exponential decay. This shape can be described by: Figure 3.1 c

$$f(t) = (1-e^{-\alpha t})\, H(t) + (1-e^{-\alpha \tau})\, H(t-\tau) \qquad (3.5)$$

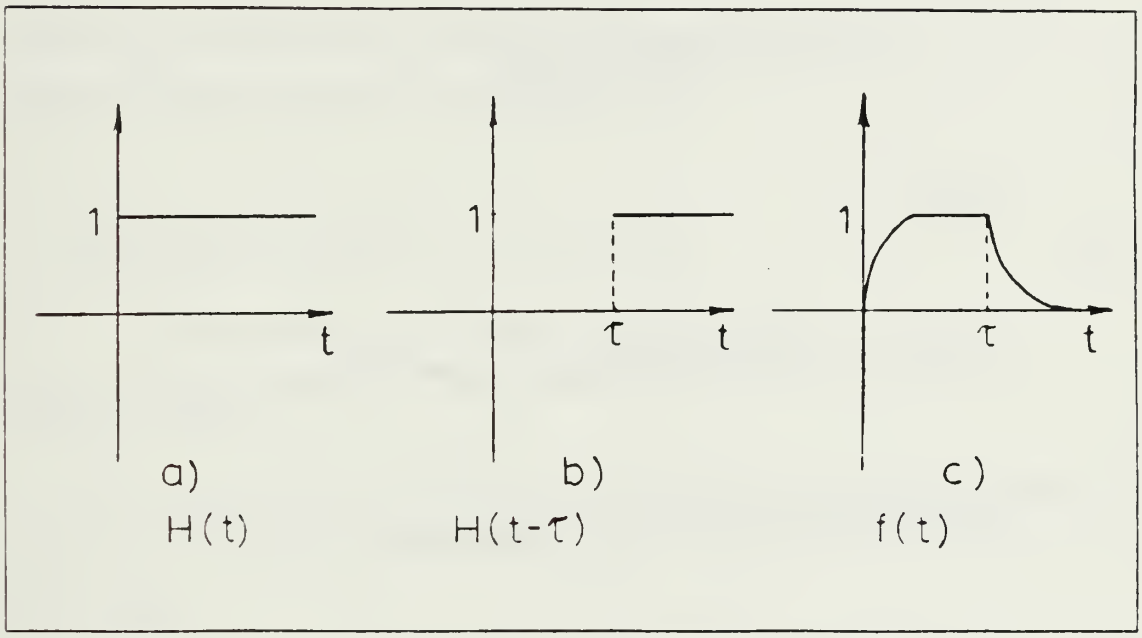

Figure 3.1 Step unit function and transmitted acoustic pulse.

Where t is the time measured from the beginning of the pulse and α the rise and decay constants. For a transducer located in the water sending pulses towards a smoothed surface the intensity received by the same transducer must be according to Chang (1986)

$$I = [\int T_i^2\, s_v\, e^{-\beta\xi}\, I_o\, f(t-2\xi/c)d\xi/(r+\xi)^2 + R_i I_o/r^2]/r^2 \qquad (3.6)$$

where:

T_i = intensity transmission coefficient

β = absortion cofficient in the sediment = 0.25 f (Urick,1979)

ξ = affected sediment depth = $c\,\tau/2$

R_i = intensity reflection coefficient

r = distance from transducer to the sediment surface

The first term inside the square brackets represents the scattered component of the scattered intensity for the volume of the sand and the second the reflected one.

For $r >> \xi$

$$I_s = (T_i^2\, s_v\, I_o / r^4) \int e^{-\beta\xi} f(t-2\xi/c)d\xi \qquad (3.7)$$

where

$$f(t-2\xi/c) = [1-e^{-\alpha(t-2\xi/c)}]H(t-2\xi/c) + [1-e^{-\alpha(t-\tau-2\xi/c)}]H(t-\tau-2\xi/c) \qquad (3.8)$$

After integration between $\xi = 0$ and $\xi = c\tau/2$

$$I_s = A\,[(1-e^{-c\beta t/2})/\beta - (e^{-c\beta t/2} - e^{-\alpha t})/(-\beta + 2\alpha/c) \qquad (3.9)$$

$$+ (e^{-c\beta(t-\tau)/2} - 1)/\beta + (e^{-c\beta(t-\tau)/2} - e^{-\alpha(t-\tau)}) / (-\beta + 2\alpha/c)]$$

where

$$A = T_i^2\, s_v\, I_o / r^4 \qquad (3.10)$$

With some algebraic operations

$$I_s = A\{1/\beta[e^{-c\beta t/2}(e^{c\beta\tau/2}-1)] \quad (3.11)$$

$$+ 1/(-\beta + 2\alpha/c)[e^{-c\beta t/2}(e^{c\beta\tau/2}-1) + e^{-\alpha t}(1-e^{-\alpha\tau})\}$$

and the reflected component

$$I_r = I_o R_i / r^4 (e^{-\alpha\tau}-1)\, e^{-\alpha t} \quad (3.12)$$

Adding the two components incoherently, the total (reflected and scattered) intensity received by the transducer will be

$$I = B\{T_i^2 s_v/\beta[e^{-c\beta t/2}(e^{c\beta\tau/2}-1) + T_i^2 s_v/(-\beta + 2\alpha/c) \quad (3.13)$$

$$[e^{-c\beta t/2}(e^{c\beta t/2}-1) + e^{-\alpha t}(1-e^{-\alpha\tau})] + R_i(e^{-\alpha\tau}-1)e^{-\alpha t}\}$$

where $B = I_o/r^4$

The expression looks quite complex but all the variables are known except s_v. If the part included inside braces is called C, then

$I = (I_o/r^4)\, C$

The quantity inside brackets is the received intensity considering only spherical spreading and C accounts for the scattered and reflected intensity. The only interesting part is for $t > \tau$, that corresponds to the decay portion. That is also what is measured in the experiment, i.e. the decay of the pulse tail.

To find the value of s_v, Chang combined the expression for C with his experimental results. Guessing values for s_v, the corresponding values for C were obtained. He repeated then the arithmetic procedure until the value of the log $C^{1/2}$ that expresses the slope decay became close to the decay constant obtained experimentally. The value guessed for s_v is then the volume scattering coefficient for the sediment studied.

This simple model appears to approximate the volume scattering. Further study of volume reverberation from ocean sediments to improve the model was thus suggested.

IV. EXPERIMENT

A. INSTRUMENTATION

1. Experiment Environment

All of the preliminary and main experiments were conducted in two steel-bound glass tanks filled with fresh water and having interior measurements of 0.7 m by 0.7 m by 0.6 m. Four different materials, *fine sand*, *aquarium sand*, *aggregate* and *glass beads*, were placed at the bottom of the tank to serve as "sediments".

The tank had 0.35 m of water overlying a 0.25 m thick layer of "sediment". Specifically, the *aggregate* and the *glass beads* were kept inside a plastic bucket during the experiment to reduce the amount of material used. Because the transducer beam is narrow (projected spot is a circle with 0.1 m radius at a 0.3-m range), the beam fell completely inside the bucket (Figure 4.1).

The *fine sand*, also studied by Bradshaw (1981), Diaz (1986) and Chang (1986), had an average size of 0.3 mm and varied from 0.15 mm to 0.7 mm. The *aggregate*, also used by Diaz (1986) and Chang (1986), was less homogeneous in size and composition than the *fine sand* and had an average size of 5.3 mm.

It was convenient to make measurements using a sediment size between 0.3 mm and 5.3 mm for a better evaluation of the volume reverberation behavior with the grain sediment size, and for that a third sediment was selected, the *aquarium sand*. This one was sieved and sized to an average size of 1.72 mm and varied from 0.84 mm to 3.36 mm with many inhomogeneities in composition and shape. It was expected that these variations in size, shape and constitution for the same sediment would raise some difficulties and this was confirmed during the experiment. The idea of performing the experiment on an ideal homogeneous sediment lead to the use of spherical *glass beads*, whose density (2.5 g/cm^3) is not far from the real sediments' densities and size is 1.7 $\pm$ 0.3 mm.

The four different materials, namely the *fine sand*, the *aggregate*, the *aquarium sands* and the *glass beads*, were kept in water for two to three days before measurements were made. A water jet from a hydraulic pump, or manually stirring was used to remove trapped air bubbles before and during the measurement process. Bleach was added to the water to control biological growth, and a wetting agent was also mixed with water to help remove air bubbles.

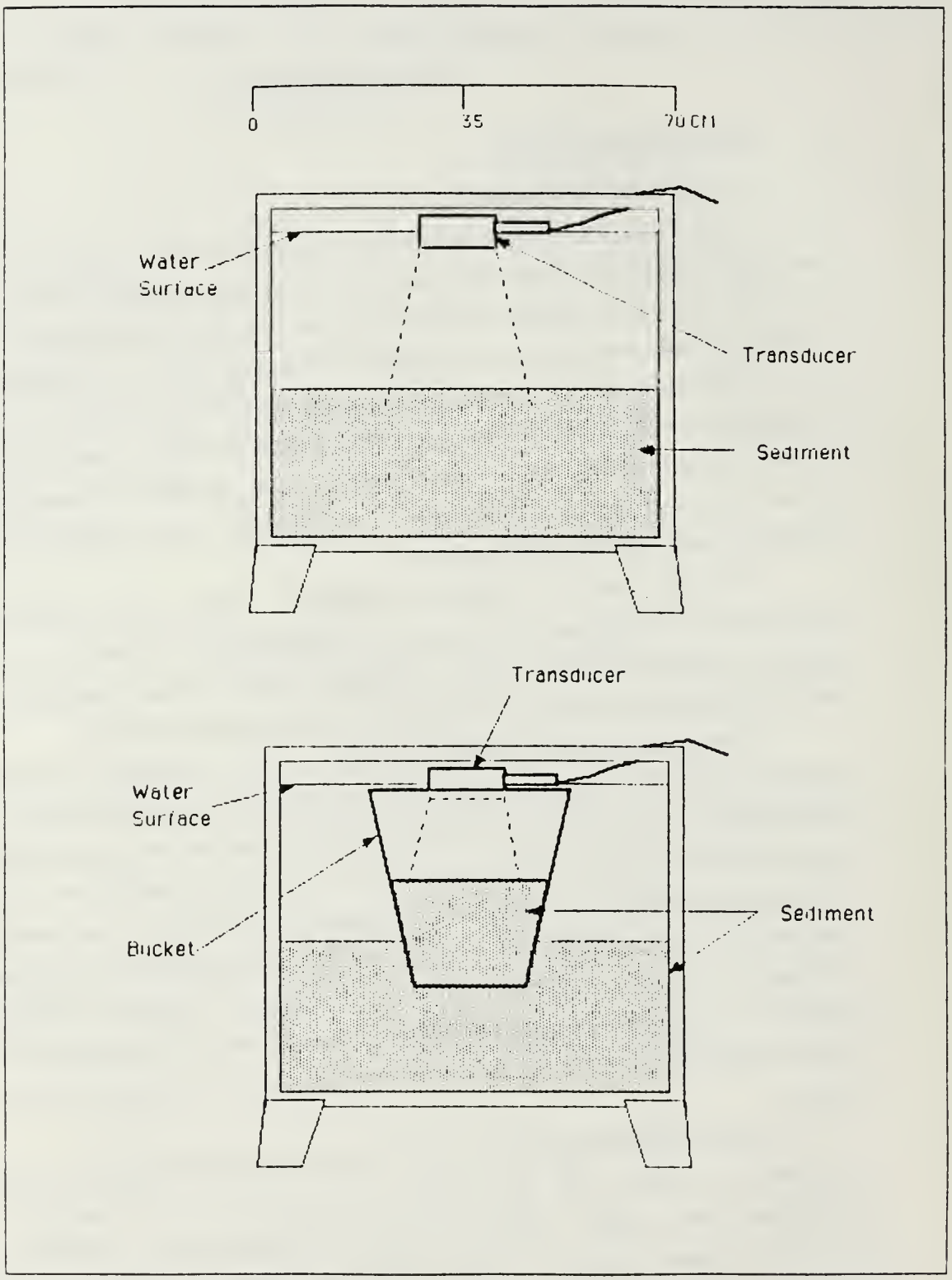

Figure 4.1 Experimental Geometry Design.

2. **Electronic Equipment**

A General Radio Model 1310 Oscillator generated a 181-kHz signal that was simultaneously fed into a frequency counter and a General Radio type 1396-A Tone Burst Generator to produce a 16-cycle pulse, which was then amplified by a Hewlett Packard 467A power amplifier before passing to a Datasonics Transmit/Receive (T/R) switch that controlled the transmission and reception by the same transducer. The transmitted signal was used to trigger an analog oscilloscope (Tektronix Type RM 503) and a Nicolet model 3091 Digital oscilloscope.

The transducer, a Naval Research Laboratory F-41 circular piston type with an 8.8-cm diameter active face, has a resonance frequency of 182 kHz and a half-beam width of 10 degrees (Diaz,1986).

The signal received by the transducer was amplified 20 dB by a 465A Hewlett-Packard pre-amplifier and then filtered by a Spencer Kennedy Laboratories, Inc. Model 302 electronic filter, used as a high pass filter to avoid low frequency noises. The filtered signal was finally passed to the oscilloscope which was controlled by a 3421A Hewlett Packard Data Acquisition/Control unit attached to an Hewlett Packard 86 desk-top computer.

All the equipment worked reasonably well : The frequency generator showed a drift of ± 150 Hz during a complete set of 10 measurements, but this did cause any significant changes in the pulse waveform, as long as the transducer was operated near its resonance. The digital oscilloscope was controlled by the computer and the the data acquisition/control unit, but sometimes during the measuring process the oscillioscope stayed locked in the STORE mode making it necessary to interrupt the measurements and reset it.

Each set of measurements was the result of 50 samples and took about 45 minutes. A faster sampling rate could speed up the measuring process and probably give us a more accurate waveform reconstitution. A block diagram of the equipment is shown in Figure 4.1.

B. PRELIMINARY MEASUREMENTS

Preliminary measurements of density, speed of sound and reflection coefficient were made for later computations of acoustic characteristics.

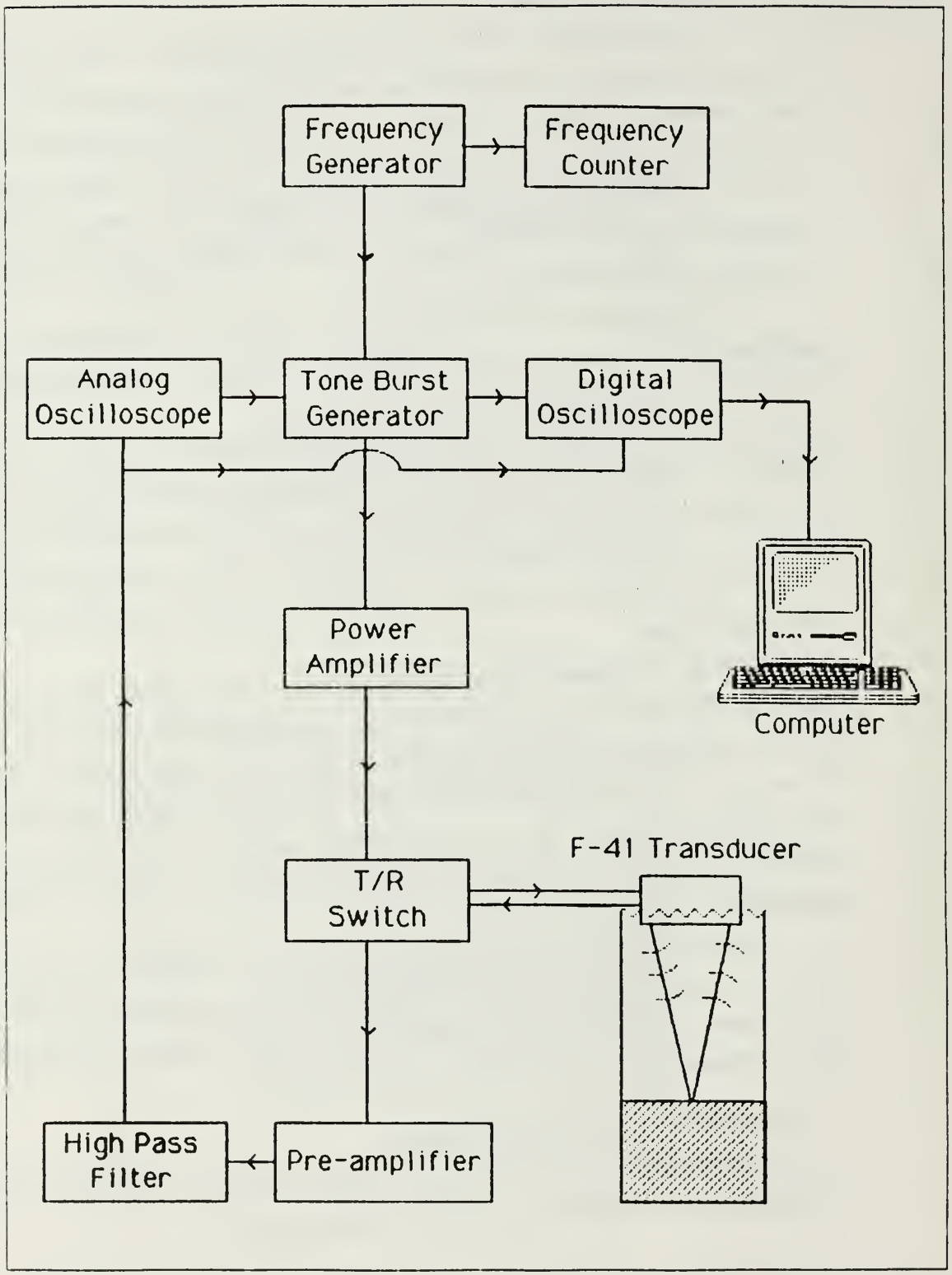

Figure 4.2 Electronic Equipment block diagram.

1. **Density**

Bradshaw (1981) measured the water-saturated density, ρ_{mix}, and dry density, ρ, of *fine sand* and obtained:

$\rho_{mix} = 1.98 \pm 0.03$ g/cm^3

$\rho = 2.69 \pm 0.01$ g/cm^3

For the *aggregate* Diaz (1986) obtained :

$\rho_{mix} = 1.97$ g/cm^3

$\rho = 2.64$ g/cm^3

Density measurements were also performed for the *aquariumsand* and for the *glass beads*. The results are summarized in Table 1.

2. **Speed of Sound**

The measurement of sound speed in the sediment was performed inside the glass tank using three LC10 transducers, one acting as a transmitter and the other two as receivers. The transducers were buried in the sediment at the same depth. The transmitter and the closest receiver were kept fixed and the third transducer was moved to different positions along the line connecting the first two transducers.

The difference in reception time at the two receivers was measured by means of the digital oscilloscope (Figure 4.3), and by measuring the distance between the receivers it was possible to calculate the sound speed. Fifteen measurements were made on the *aquarium sand* resulting in $c = 1588 \pm 22$ m/s.

Hamilton et al. (1956) studied the physical properties of marine sediments from off the coast of San Diego, California, and established some relations between the sediment grain sizes and their physical properties such as porosity, density, speed of sound, etc. They observed a general increase of sound speed with increase in medium grain size. Thus, the value of the sound speed for the *aquarium sand* was smaller than the 1610 m/s obtained by Bradshaw (1981) for the *fine sand*, and does not agree with Hamilton et al.. the last conclusion. To investigate the consistency of that value, a second set of measurements was made and the result was $c = 1590 \pm 42$ m/s, confirming the first one.

The same experimental procedure was conducted on the *glass beads* and the results were $c = 1822 \pm 48$ m/s

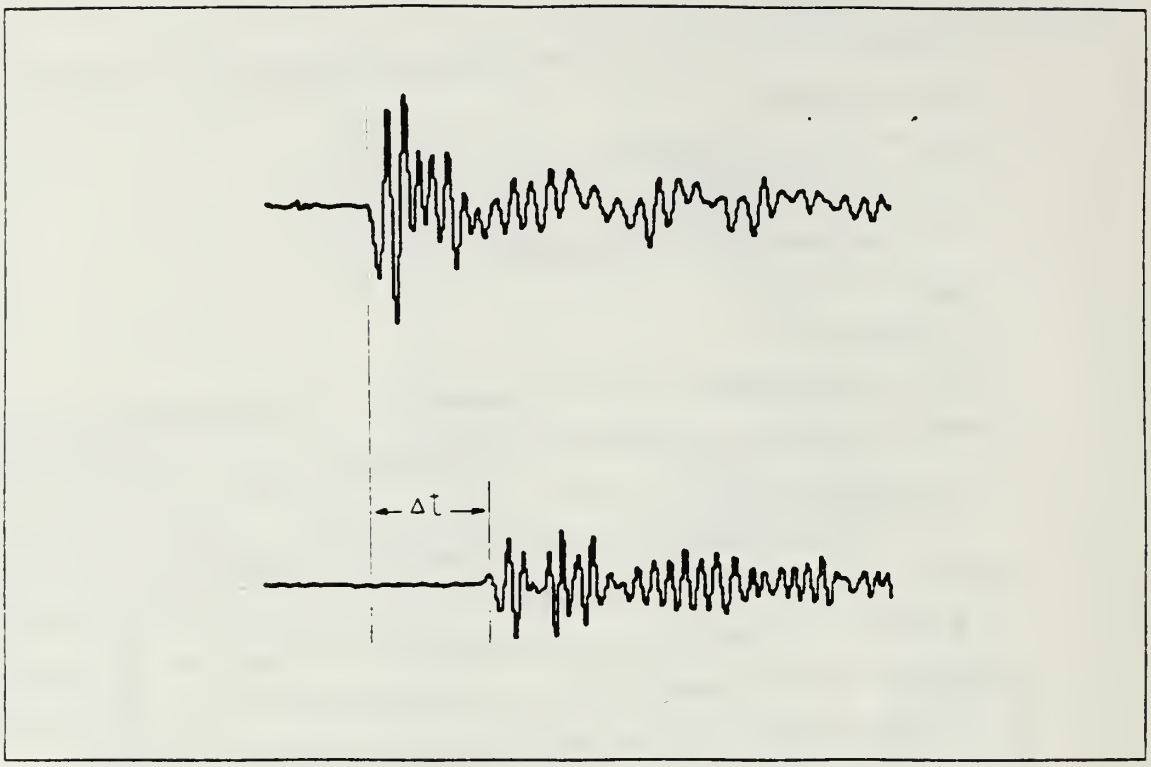

Figure 4.3 Detail of speed of sound measurement procedure.

3. **Reflection Coefficient**

The reflection coefficient for sound rays passing from one medium to another is the ratio between the reflected and the incident acoustic pressures, and for normal incidence it depends on the specific acoustic impedance ρc, of each medium. The reflection coefficients for *aquarium sand* and *glass beads* were measured as the ratio between the maximum voltage amplitude in the signal reflected from the sediment and the signal reflected by the water-air interface at the same distance.

$$R = V_r/V_i \tag{4.1}$$

The reflection coefficient can also be computed using

$$R = (r_2 - r_1)/(r_2 + r_1) \tag{4.2}$$

where

$r_1 = \rho_1 c_1$ is the specific acoustic impedance for the water

$r_2 = \rho_2 c_2$ for the sediment

The measured, R_m, and computed, R_c, values of the reflection coefficient, as well as other physical characteristics are summarized in Table 1.

TABLE 1

SEDIMENT PHYSICAL CHARACTERISTICS

	fine sand	aggregate	aquarium sand	glass beads
a (mm)	0.3 (± 0.3)	5.3 (± 0.51)	1.72 (± 0.24)	1.7 (± 0.3)
ρ (g/cm^3)	2.69 (± 0.01)	2.64 (± 0.05)	2.59 (± 0.05)	2.50 (± 0.05)
ρ_{mix} (g/cm^3)	1.98 (± 0.03)	1.97 (± 0.05)	2.02 (± 0.02)	1.91 (± 0.01)
c (m/s)	1610	1555	1588 (± 22)	1822 (± 48)
R_m	0.36	0.36	0.36 (± 0.09)	0.53 (± 0.05)
R_c	0.38	0.52	0.38 (± 0.01)	0.41 (± 0.01)

C. MEASUREMENT PROCEDURES

1. Experiment Technique

To measure the exponential decay of the tails of the pulses scattered from the sediment the experimental procedure of Diaz (1986) and Chang (1986) was used. The transducer was clamped to a horizontal wooden rail that kept the transducer level with its active face pointing downward to the sediment as shown in Figure 4.1.

In his experiment Chang observed large variations in the received pulse shapes between different samples of the same sediment and concluded that the variations were due to inhomogeneities in the sediment. Because of this, he did not obtain consistent results. To smooth the variations in the results a set of ten measurements was performed with various transducer positions, and the results were averaged

For the *aggregate sand* it is not difficult to accept that important inhomogeneities are present in its components, but the *fine sand*, looks quite homogeneous. However, the waveforms did show large variations. By performing the experiment using a thin metal plate covering the sediment, Chang showed that those inhomogeneities were interior to the sediment.

To investigate these facts further, the first experiment performed in this present work consisted of keeping the transducer in a fixed position and, between each measurement the sediment was stirred using a water jet produced by a pump. During this stirring process clouds of air bubbles were released from within the sediment, and after that, the sediment texture changed completely, becoming much "silkier" to the touch.

The reflected signals then became consistent, as can be seen in Figure 4.4, where pulses scattered from this sediment, after each stirring, are displayed. The inhomogeneities found by Chang in his experiment appear to have been caused by occluded gas within the sediment. Thereafter, each sample of sediment being studied was stirred periodically, to remove any air bubbles.

2. Measurement Considerations

The measurements made on the *aquarium sand* with this new tecnique still revealed some variation, mostly in the last part of the pulse tails, as can be seen in the group of five waveforms in Figure 4.5 and in the measured decay slopes presented in Chapter 5.

Measurements for the *aggregate* were repeated to determine if the inconsistencies in our results were also due to the presence of gas bubbles within the

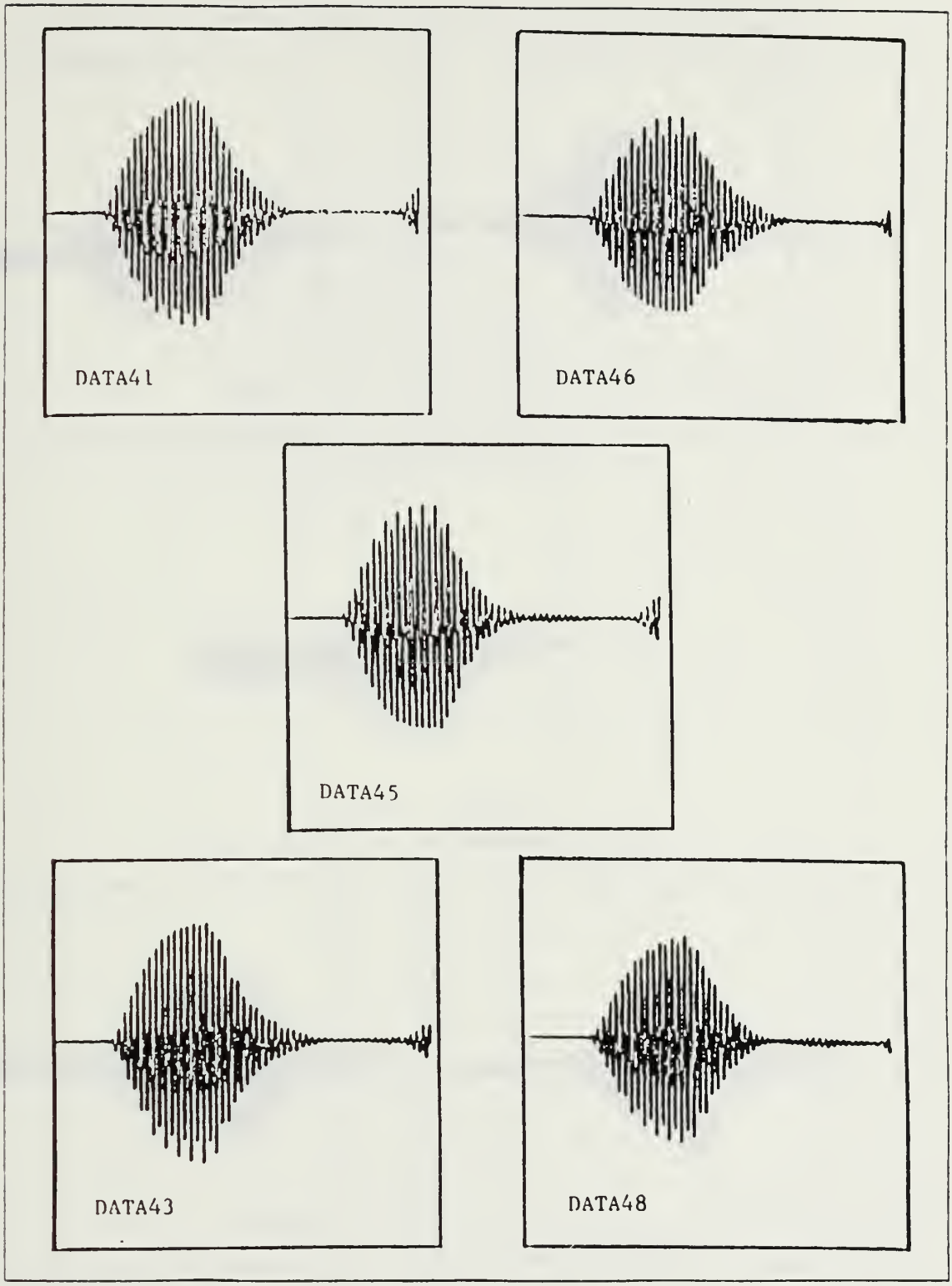

Figure 4.4 Waveforms of pulses scattered from fine sand.

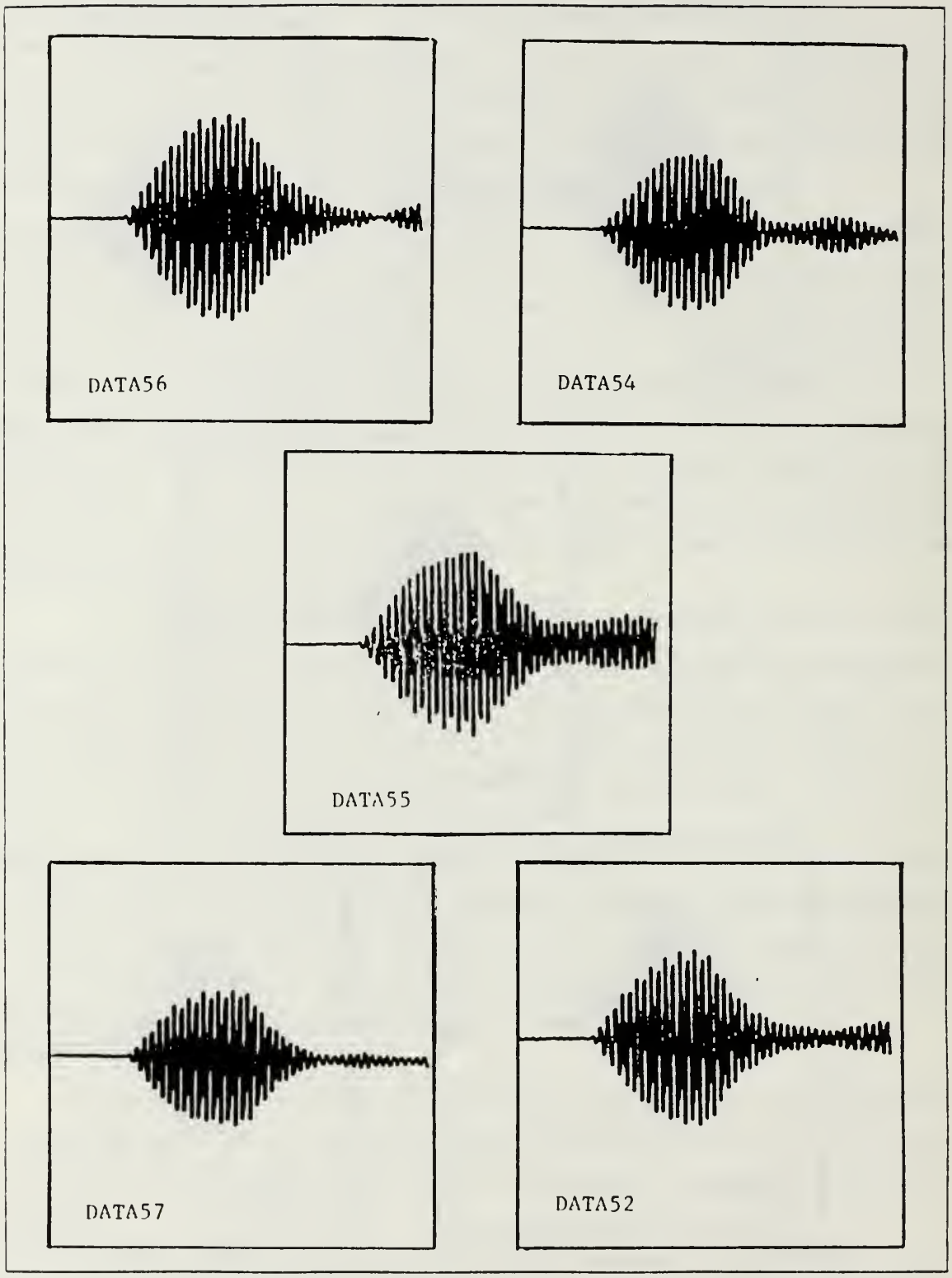

Figure 4.5 Waveforms of pulses scattered from aquarium sand.

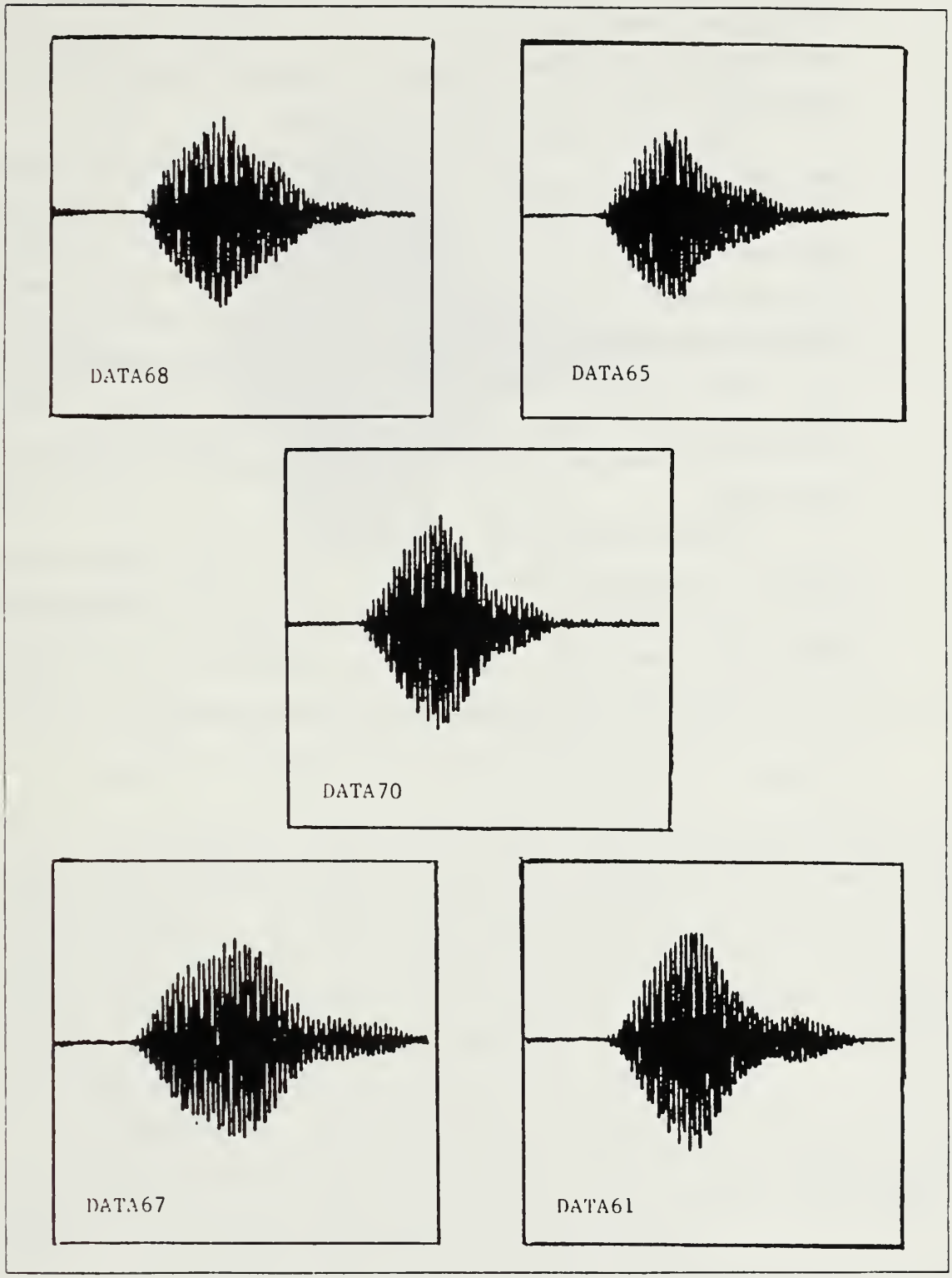

Figure 4.6 Waveforms of pulses scattered from aggregate.

sample or due to the visible physical inhomogeneities present. This time, the variations remained (Figure 4.6) although when the sediment was deeply stirred only a few bubbles were observed during the stirring. A conclusion can be drawn from these experiments with the different sediments : The variations in the tail shape of the pulse increases as the grain size of the sediment increases.

The consistent dependence of the results on the grain size, indicated that we may have been working with grain dimensions too large relative to the wavelength. In fact the average dimension of the *aggregate* is 5.3 mm and the wavelength is 8 mm, values that are very close. One of the assumptions necessary to determine the volume reverberation is that the surface scattering is negligible, because the sediment surface is levelled and smoothed. The levelling of the bottom surface was made by using a device that, rolling on the tops of the tank walls, produced a horizontally levelled bottom surface. Even with levelling, when the grain sizes are relatively big there is always a gap between adjacent grains that destroy the smoothness and produces the effect of a rough surface.

A simple experiment was performed to determine the importance of surface scattering. A Styrofoam plate, to simulate a pressure release interface was weighted down on the sediment surface and covered by a thin layer of sediment, and the scattered pulses were analysed. In this case, any changes in the pulse waveforms would result, not from volume reverberation, but from surface scattering.

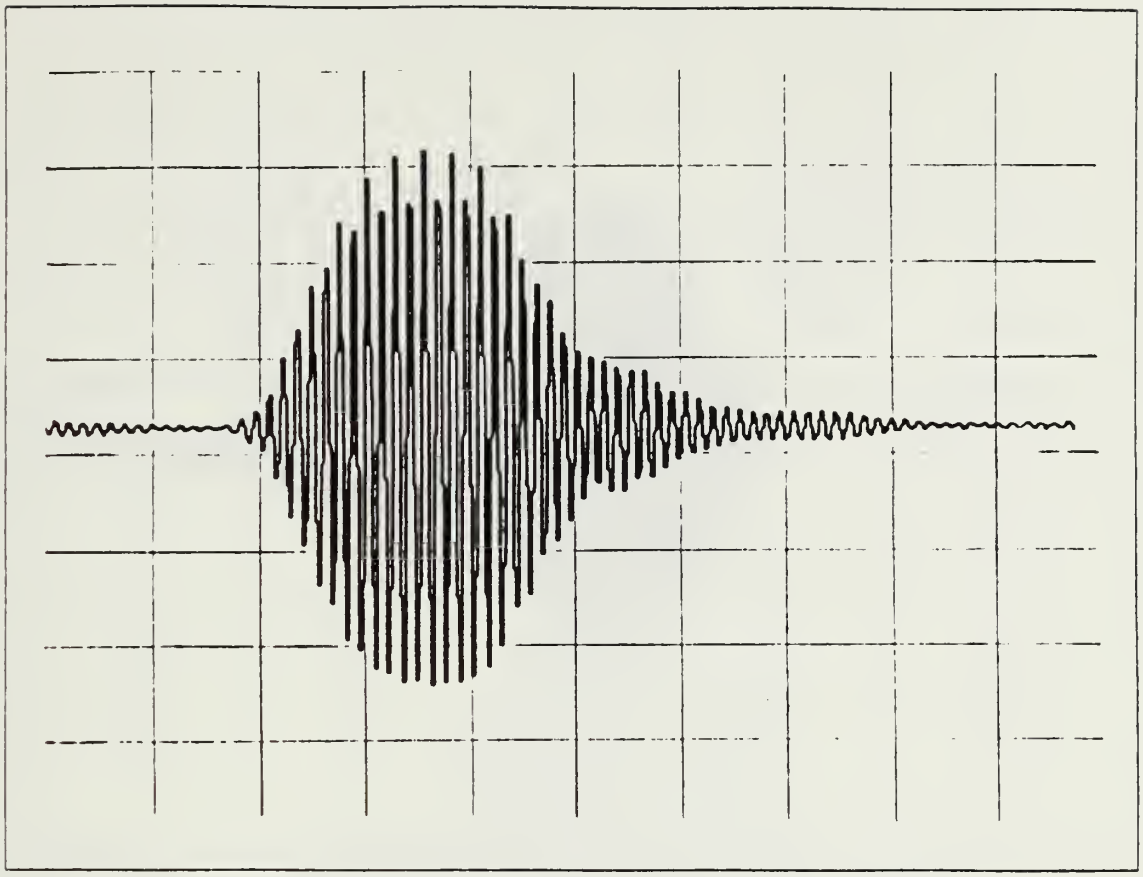

Figure 4.7 Waveform of pulse reflected from a thin layer of aggregate.

It was sufficient to observe the waveform on the oscilloscope to find that the decay changed drastically each time the transducer was slightly moved. Merely moving some grains from the thin layer caused the received pulse to change completely. The pulses (Figure 4.7 to Figure 4.9) showed many of the same features as were observed during the volume reverberation measurements. It was concluded that surface scattering was a significant factor in reflection from sediment when the grain size was comparable to the wavelength of the sound.

Performing the same experiment with *Aquarium sand* led to a similar conclusion that surface scattering was playing an important role. Although the pulse waveforms did not show large variations, the values for the decay slopes showed a significant spread, indicating the presence of surface scattering.

To analyse the extent of the influence of inhomogeneities on the results obtained in the measurements performed with the three previously indicated sediments,

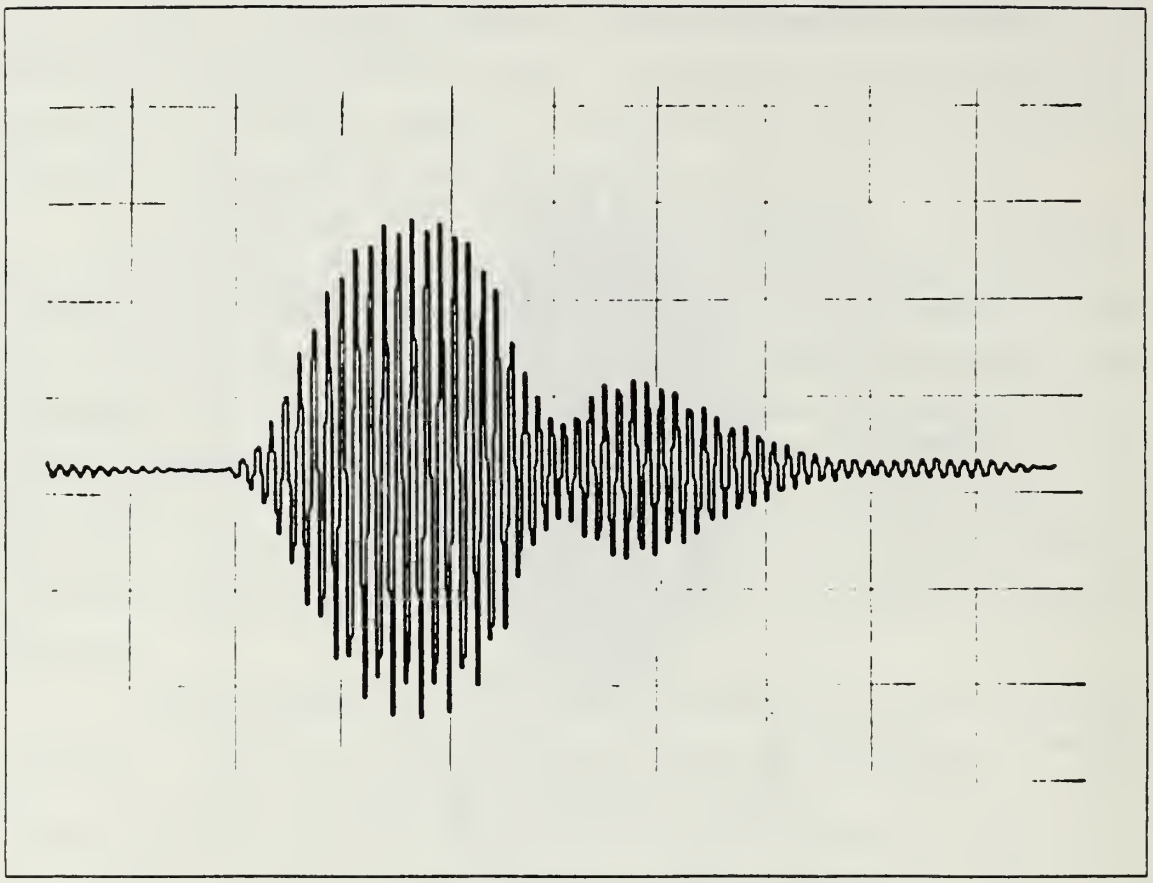

Figure 4.8 Waveform of pulse reflected from a thin layer of aggregate.

another set of ten observational runs was made using *glass beads*. It was expected that the reflected pulses could be more consistent due to their homogeneity. This did not happen, however, and Figure 4.11 shows five different waveforms reflected by the *glass beads*. They present approximately the same features as the pulses reflected by the *aquarium sand* whose average grain size is close to that of the beads dimensions, showing once more the influence of the grain size in its scattering properties.

3. **Data Processing**

The computer programs used in this project were designed and tested by Chang (1986). They were used to obtain the average slope for each sample:
THESIS3 is a program designed to convert and normalize the waveform data obtained from the Nicholet digital oscilloscope. Since the pulses contain positive and negative values, these are squared and a series of fifty waveform samples are averaged to give an accurate representation of the waveform envelope. Because of jitter in the trigger

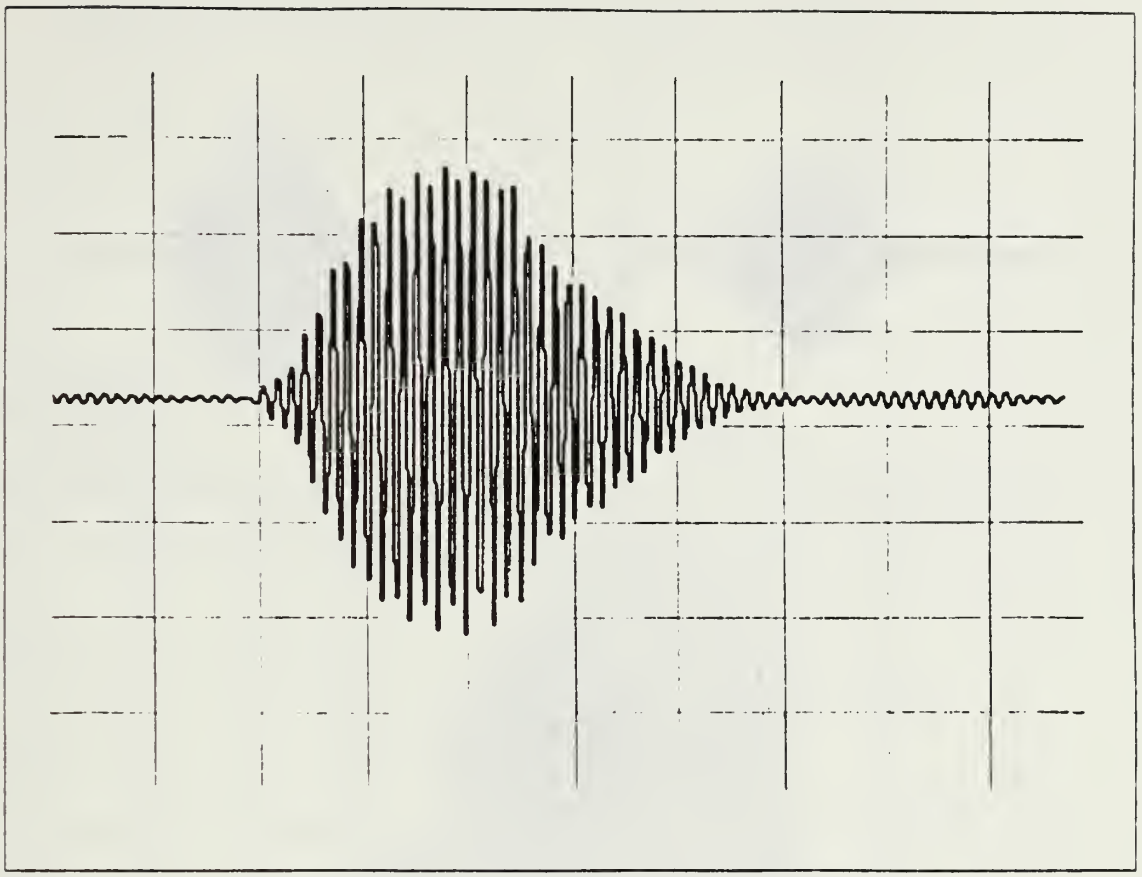

Figure 4.9 Waveform of pulse reflected from a thin layer of aggregate.

signal, each "bin" of the scope will sample the waveform at various times during a cycle, and the resulting curve will be a representation of the envelope of the pulse.

The result can be seen in Figures 4.12 to 4.14 where four tails of the puises reflected from the three different sediments are plotted.

MAXIMUM is a program used to choose the local maxima for the curves obtained from THESIS3 stored on disk. The square root of these maxima is then taken and stored in the same disk. The result is shown in Figures 4.15 to 4.17 which show respectively the envelopes of the pulse tails shown in Figure 4.12 to Figure 4.14.

PLOT3 is used to produce the plots of the waveform envelopes and to apply a least square method to find the best fitted straight line, its slope and correlation coefficient.

AVERAGE. The measurement of the slope of the tail was very sensitive to any change in the sediment sample, and to get a consistent result ten sets of measurements were performed, and this program is applied to compute a chain average in the following way:

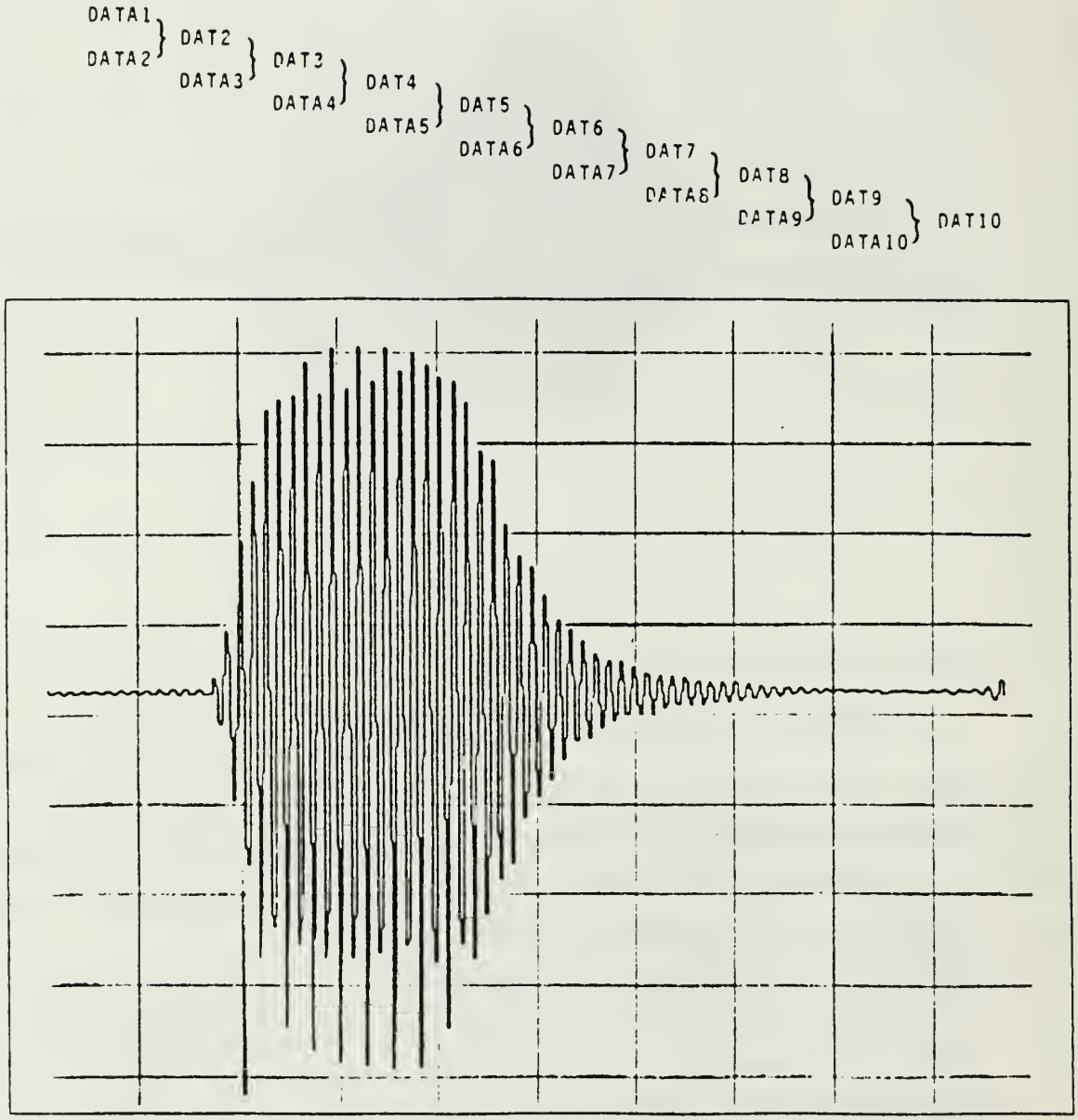

Figure 4.10 Waveform of pulse reflected from Styrofoam plate.

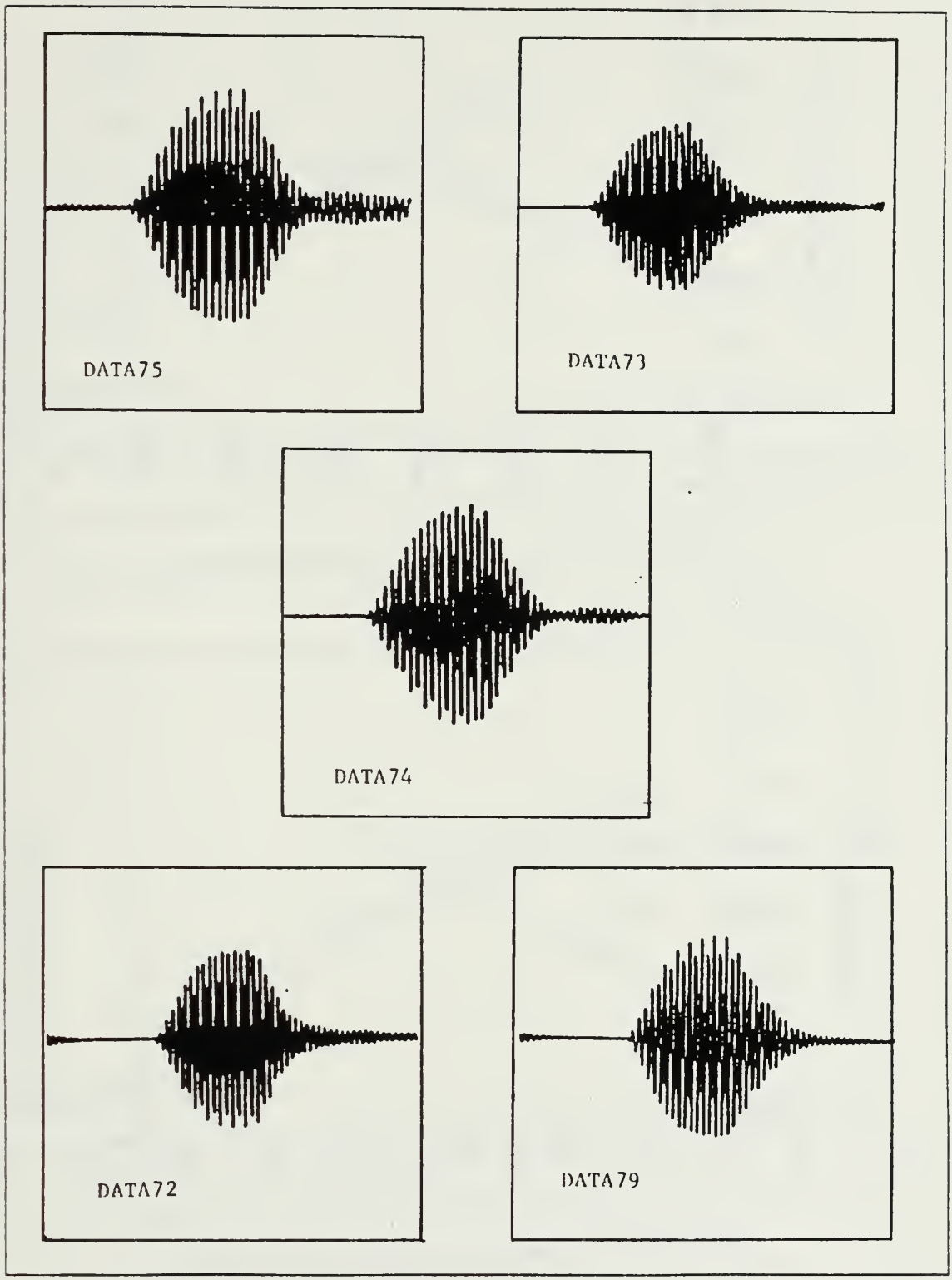

Figure 4.11 Waveform of pulses scattered by glass beads.

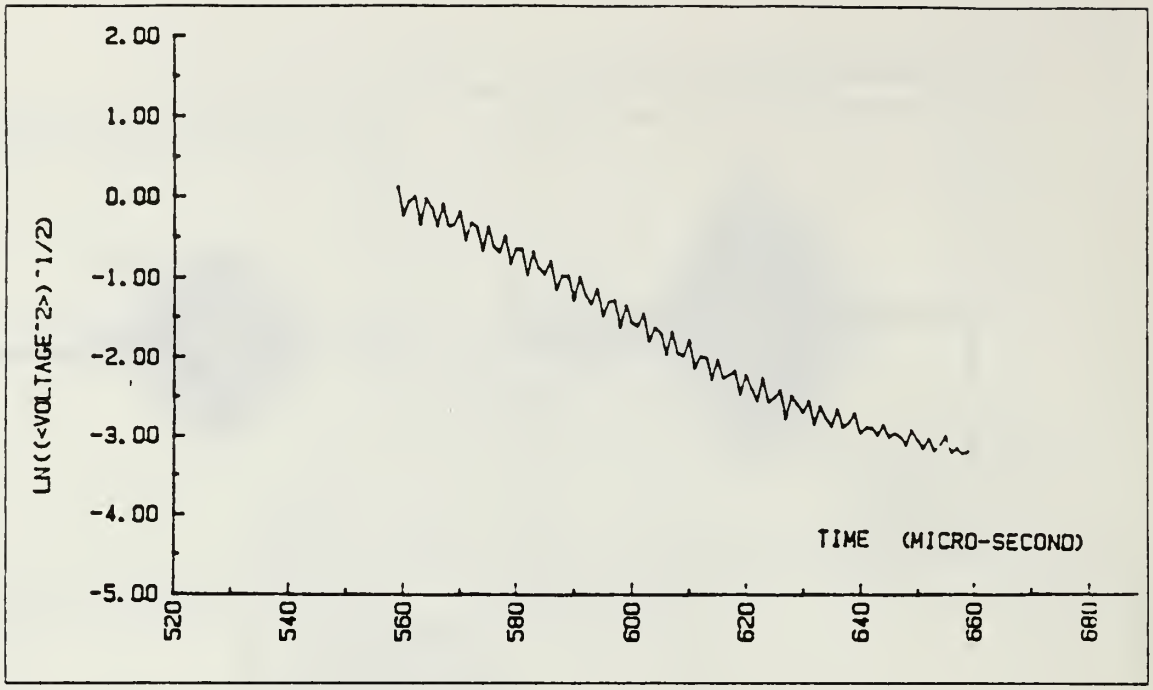

Figure 4.12 Tail waveform of pulse reflected from fine sand.

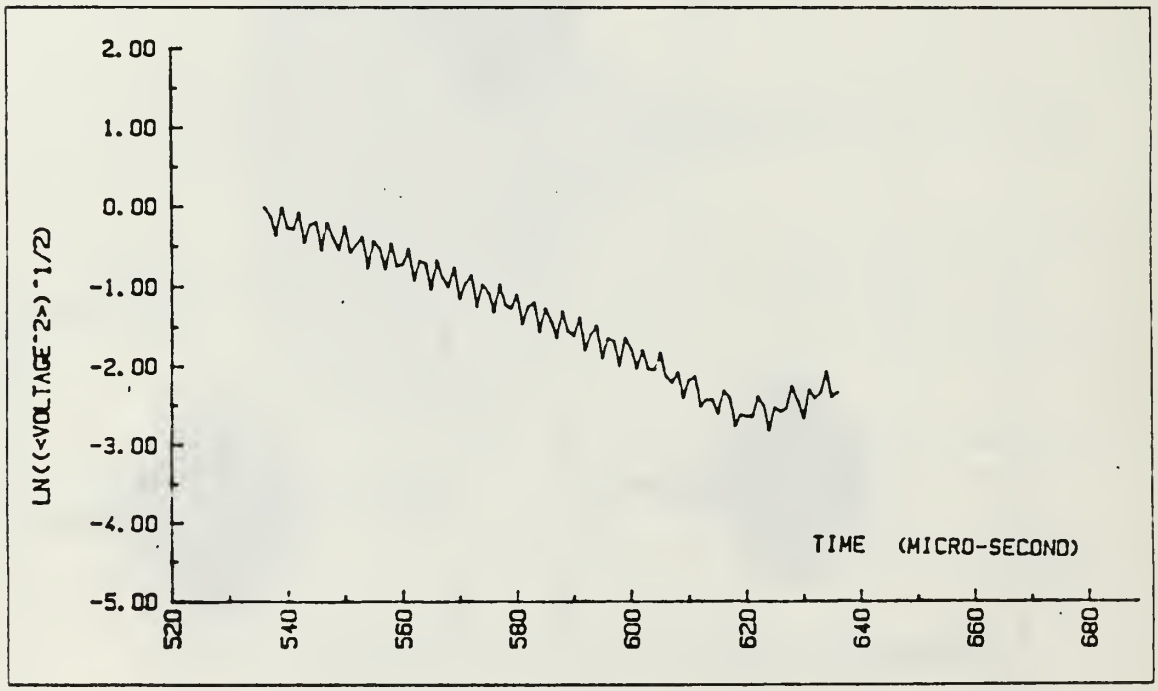

Figure 4.13 Tail waveform of pulse reflected from aquarium.

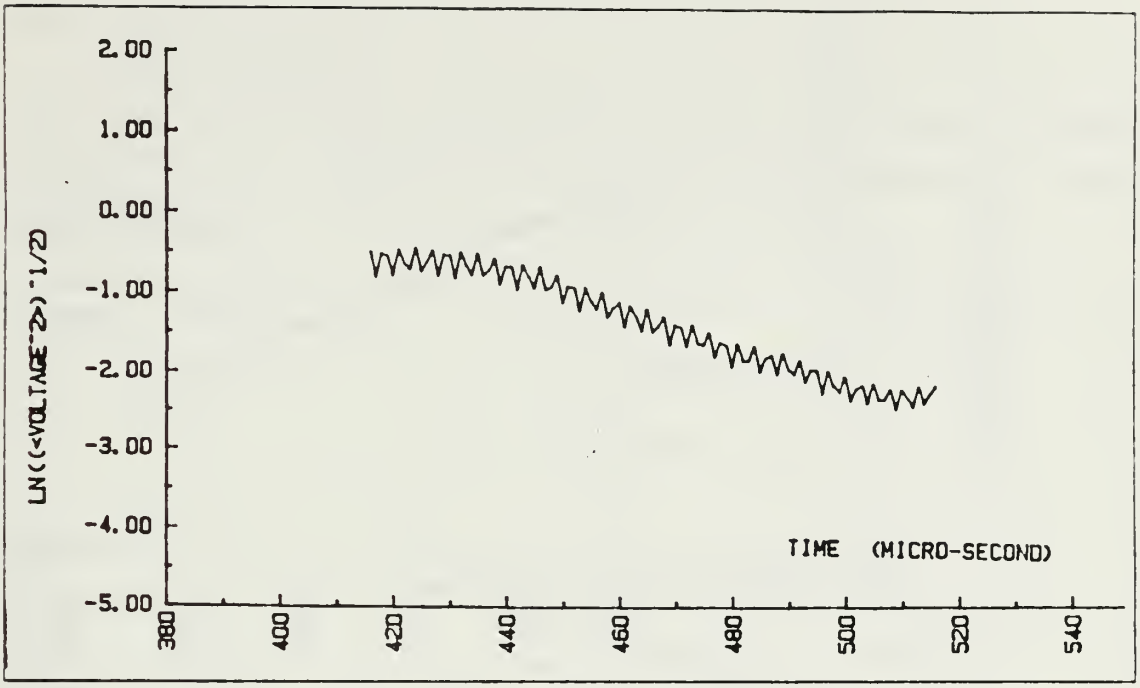

Figure 4.14 Tail waveform of pulse reflected from aggregate.

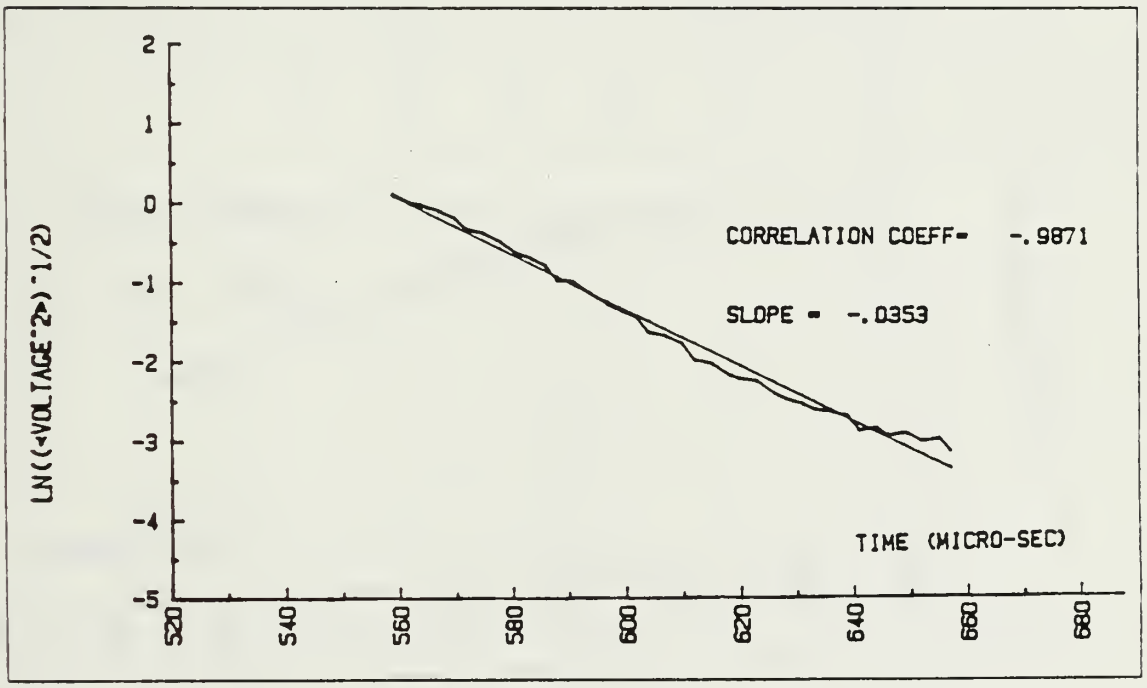

Figure 4.15 Tail envelope of a pulse reflected from fine sand.

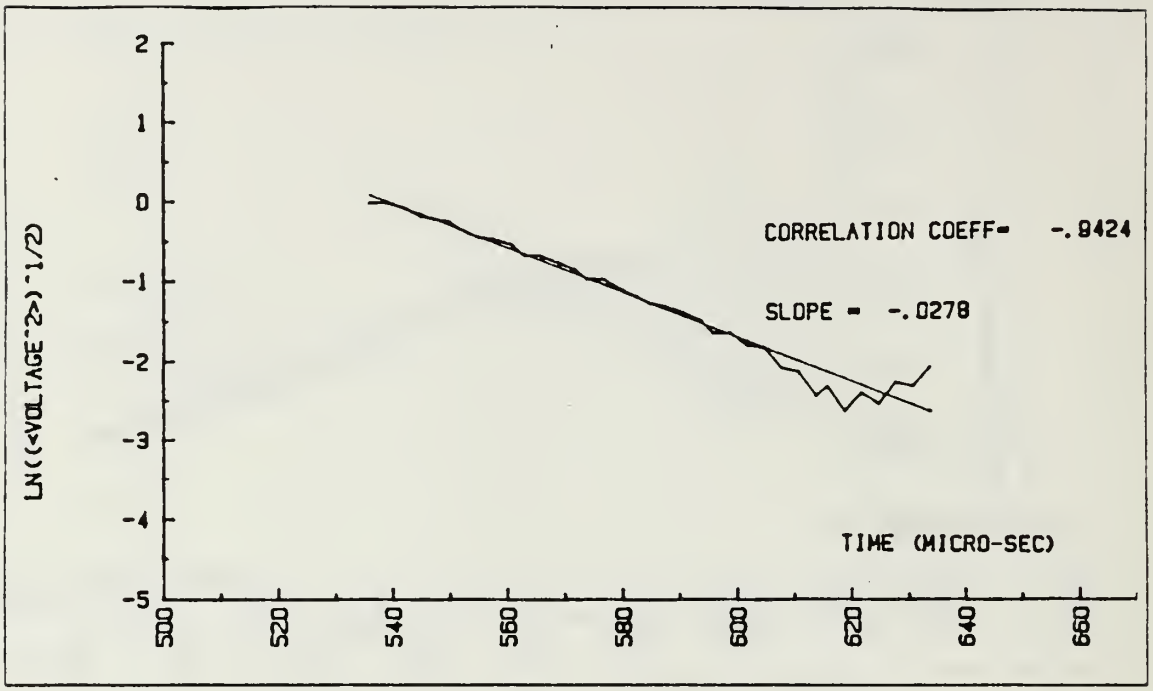

Figure 4.16 Tail envelope of a pulse reflected from aquarium.

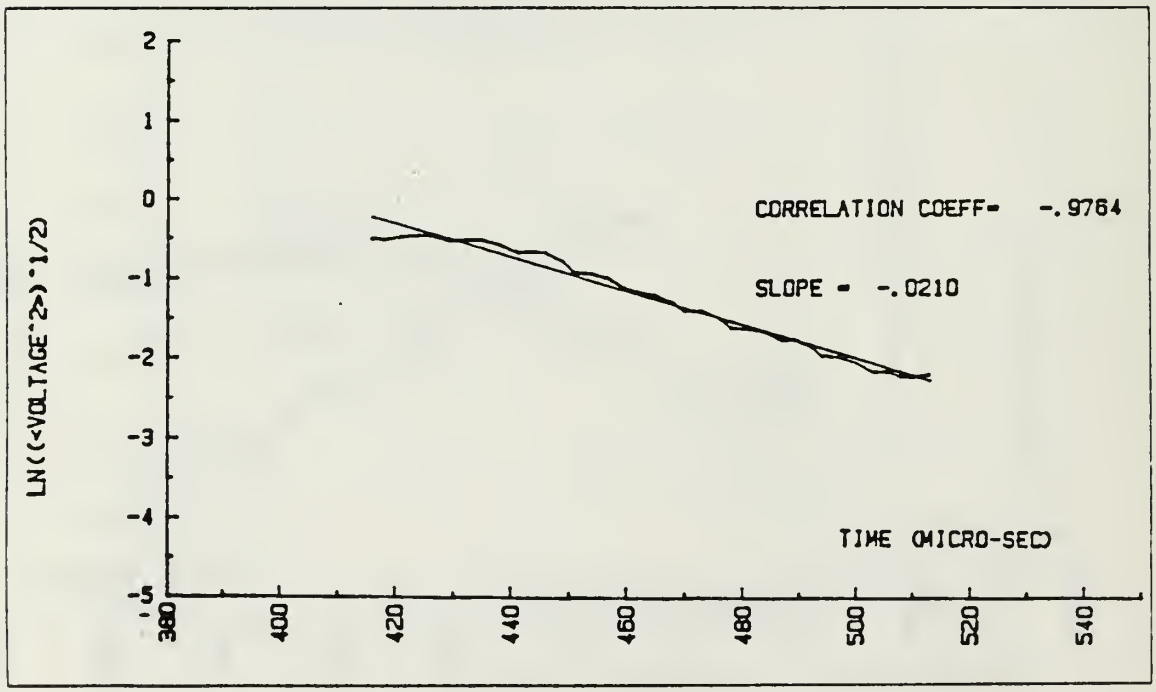

Figure 4.17 Tail envelope of a pulse reflected from aggregate.

Each averaging step is divided by the number of terms envolved so that each data set has the same weight. The DAT10 is then the file that contains the averaged maxima that plotted in Figure 4.18 shows a much more regular envelope than the envelopes of the local maxima plotted, for example, in Figure 4.12.

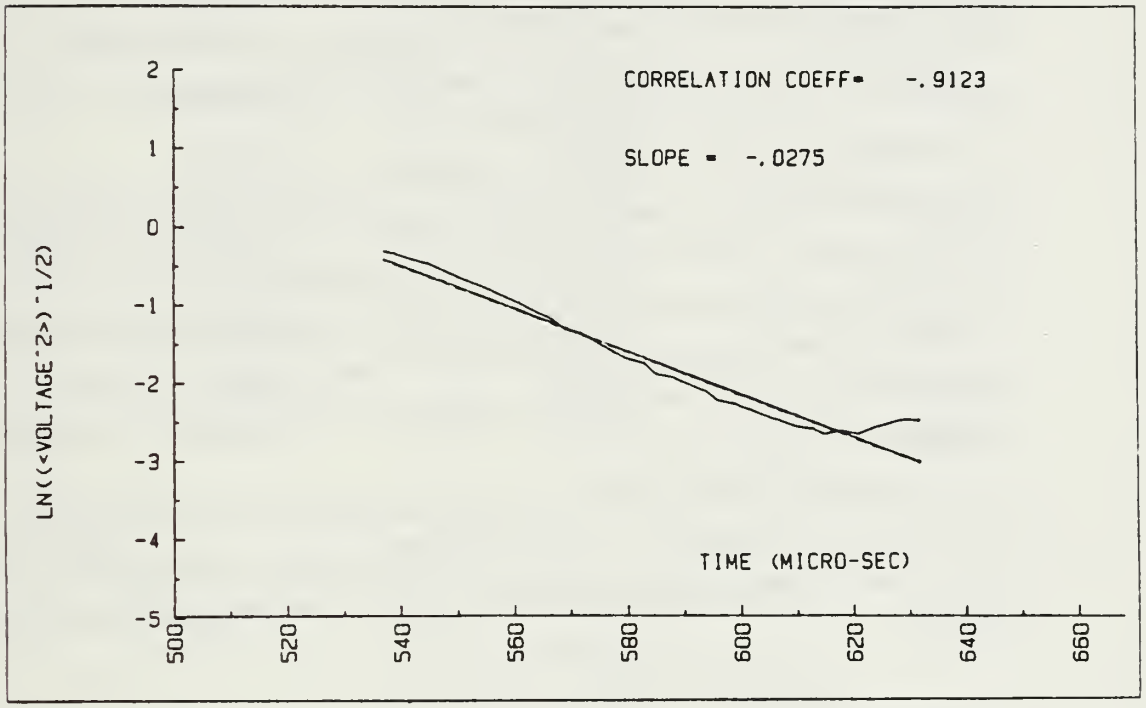

Figure 4.18 Final envelope of an averaged pulse.

V. RESULTS

The decay constants of the trailing edge of sound pulses reflected off the bottom may be used to determine the volume reverberation of bottom material. However, the volume reverberation obtained is quite sensitive to inhomogeneities in both small-scale bottom topography and sediment composition.

In fact, even very homogeneous surfaces, such as the air -water interface led to slope small fluctuations between successive runs. For this reason, averages of several runs were used to determine the volume reverberation level. The use of an average of several runs becomes even more important when the sediment grain size increases.

In the results presented next, this fact is very evident. In Figure 5.1, the decay constants obtained for the different sediments show big fluctuations mainly for the aggregate and aquarium sand.

A proportionality between the sediment grain size and the amount of volume reverberation was expected as suggested by Clark, Proni, Seem and Tsai (1984). This was observed by the averaged final values of the slopes obtained for the four different sediments.

A. FINE SAND

For the fine sand, eight measurements were made and the individual slopes are listed in Table 2. For each slope, the correlation coefficient was also computed.

Despite the relative stability of the individual slopes, the chain average was applied to the 8 measurements and the results are listed in Table 3.

The running average of all eight data sets is $\eta = 3.51 \times 10^{-2}$ Np/μs and when compared to the decay constant of the purely reflected (water-air interface) pulse, $\alpha = 3.77 \times 10^{-2}$ Np/μs, shows a small amount of volume reverberation. This is justified due to the small dimensions of the grain size, (0.3 mm) compared with the 8 mm of the wavelength, making a $a/\lambda = 0.375$ which can be considered inside the Rayleigh regime.

TABLE 2
FINE SAND INDIVIDUAL SLOPES

DATA SET	SLOPE x 10^2 (Np/μs)	CORRELATION COEFFICIENT
DATA41	-3.91	-0.9731
DATA42	-3.42	-0.9162
DATA43	-3.48	-0.9611
DATA44	-3.58	-0.9682
DATA45	-3.66	-0.9575
DATA46	-3.26	-0.9526
DATA47	-3.30	-0.9485
DATA48	-3.53	-0.9871

TABLE 3
FINE SAND AVERAGE SLOPES

NO. SETS AVERAGED	SLOPE x 10^2 (Np/μs)	CORRELATION COEFFICIENT
2	-3.70	-0.9619
3	-3.66	-0.9715
4	-3.61	-0.9721
5	-3.62	-0.9765
6	-3.62	-0.9703
7	-3.50	-0.9727
8	-3.51	-0.9757

B. AQUARIUM SAND

A series of ten sets of measurements were run for this sediment (Table 4). The individual slopes present a big variation (Figure 5.1). Chain averaging gave the results in Table5.

TABLE 4
AQUARIUM INDIVIDUAL SLOPES

DATA SET	SLOPE x 10^2 (Np/μs)	CORRELATION COEFFICIENT
DATA51	-3.00	-0.7717
DATA52	-2.78	-0.9424
DATA53	-2.68	-0.7402
DATA54	-1.88	-0.6269
DATA55	-2.43	-0.9242
DATA56	-3.42	-0.9557
DATA57	-3.03	-0.9777
DATA58	-2.35	-0.8495
DATA59	-3.34	-0.8564
DATA60	-3.77	-0.9877

The final decay constant $\eta_{aq} = 2.75 \times 10^{-2}$ Np/μs is now quite different from the reference value of the water-air interface. This difference results from the effect of volume reverberation in the sediment and also, as shown in a later measurement, from surface scattering due to the relatively big dimensions of its grains compared with the wavelength ($a/\lambda = 0.25$).

TABLE 5
AQUARIUM AVERAGED SLOPES

NO. SETS AVERAGED	SLOPE x 10^2 (Np/μs)	CORRELATION COEFFICIENT
2	-3.05	-0.9634
3	-2.93	-0.9506
4	-2.53	-0.8540
5	-2.42	-0.8782
6	-2.67	-0.9003
7	-2.68	-0.9157
8	-2.68	-0.8982
9	-2.72	-0.9046
10	-2.75	-0.9123

C. AGGREGATE

Ten measurements were performed using the *aggregate* with the resulting individual slopes listed in Table 6. The variation, in the presented individual slopes is considerably larger than the variations for the *aquarium sand* (Figure 5.1), which is to be expected, since the *aggregate* shows many inhomogeneities. To make these results more understandable the chain average was run again (Table 7).

The final decay constant $\eta_{ag} = 1.84 \times 10^{-2}$ Np/μs, when compared with those for the other sediments, shows an even larger amount of reverberation in accordance with the proportionality between reverberation level and size of individual scatterers.

D. GLASS BEADS

Although the *glass beads* appear homogeneous in size, shape, and material, the individual slopes show considerable variations (Figure 5.1) with the numerical results listed in Table 8. The corresponding averaged values are presented in Table 9.

TABLE 6
AGGREGATE INDIVIDUAL SLOPES

DATA SET	SLOPE x 10^2 (Np/μs)	CORRELATION COEFFICIENT
DATA61	-2.10	-0.9764
DATA62	-3.54	-0.9385
DATA63	-2.40	-0.8392
DATA64	-2.71	-0.9772
DATA65	-1.36	-0.9322
DATA66	-2.03	-0.8901
DATA67	-2.09	-0.8187
DATA68	-1.55	-0.9313
DATA69	-1.13	-0.6211
DATA70	-1.84	-0.9612

The final decay constant for the glass beads is $\eta_g = 3.06 \times 10^{-2}$ Np/μs which is consistent with the final slopes of the other sediments, considering their relative grain sizes.

E. OVERALL RESULT

Relative values of reverberation level for the different materials are shown in Figure 5.1 The averaged values of the slopes are marked along the y-axis for the different materials. Plotting them against grain size, the corresponding best fitted straight line is defined by:

$$\eta = 3.62 - 0.0035a$$

The value of the average grain size of the sediment can then be estimated by :

$$a = 10.34 - \eta/0.0035$$

TABLE 7
AGGREGATE AVERAGE VALUES

NO. SETS AVERAGED	SLOPE x 10^2 (Np/μs)	CORRELATION COEFFICIENT
2	-2.66	-0.9476
3	-2.59	-0.9474
4	-2.62	-0.9595
5	-2.05	-0.9890
6	-2.05	-0.9736
7	-2.05	-0.9730
8	-2.00	-0.9756
9	-1.85	-0.9653
10	-1.84	-0.9719

where s is in Np/μs and a is in mm. This relationship gives only a rough estimate of the sediment grain size since, considering the standard deviations in the slopes of the extreme data points, the value for a can be estimated within ± 2.8 mm. for a slope of 2.5 x 10^{-2} Np/μs. Also this relation was established based on measurements performed using a transducer with damping corresponding to a decay constant α = 3.77 x 10^{-2} Np/μs at 180 kHz. Other transducers will have different decay constants and further measurements should be performed using different transducers to investigate the influence of α on this result.

TABLE 8
GLASS BEADS INDIVIDUAL SLOPES

DATA SET	SLOPE x 10^2 (Np/μs)	CORRELATION COEFFICIENT
DATA71	-3.48	-0.9896
DATA72	-2.92	-0.9157
DATA73	-2.99	-0.9565
DATA74	-3.03	-0.8251
DATA75	-2.10	-0.8131
DATA76	-3.22	-0.9286
DATA77	-3.81	-0.9917
DATA78	-3.40	-0.9860
DATA79	-3.94	-0.8614
DATA80	-2.92	-0.9680

TABLE 9
GLASS BEADS AVERAGED SLOPES

NO. SETS AVERAGED	SLOPE x 10^2 (Np/μs)	CORRELATION COEFFICIENT
2	-3.33	-0.9794
3	-3.19	-0.9750
4	-3.28	-0.9646
5	-2.86	-0.9421
6	-2.84	-0.9693
7	-2.83	-0.9780
8	-2.94	-0.9829
9	-3.01	-0.9789
10	-3.06	-0.9805

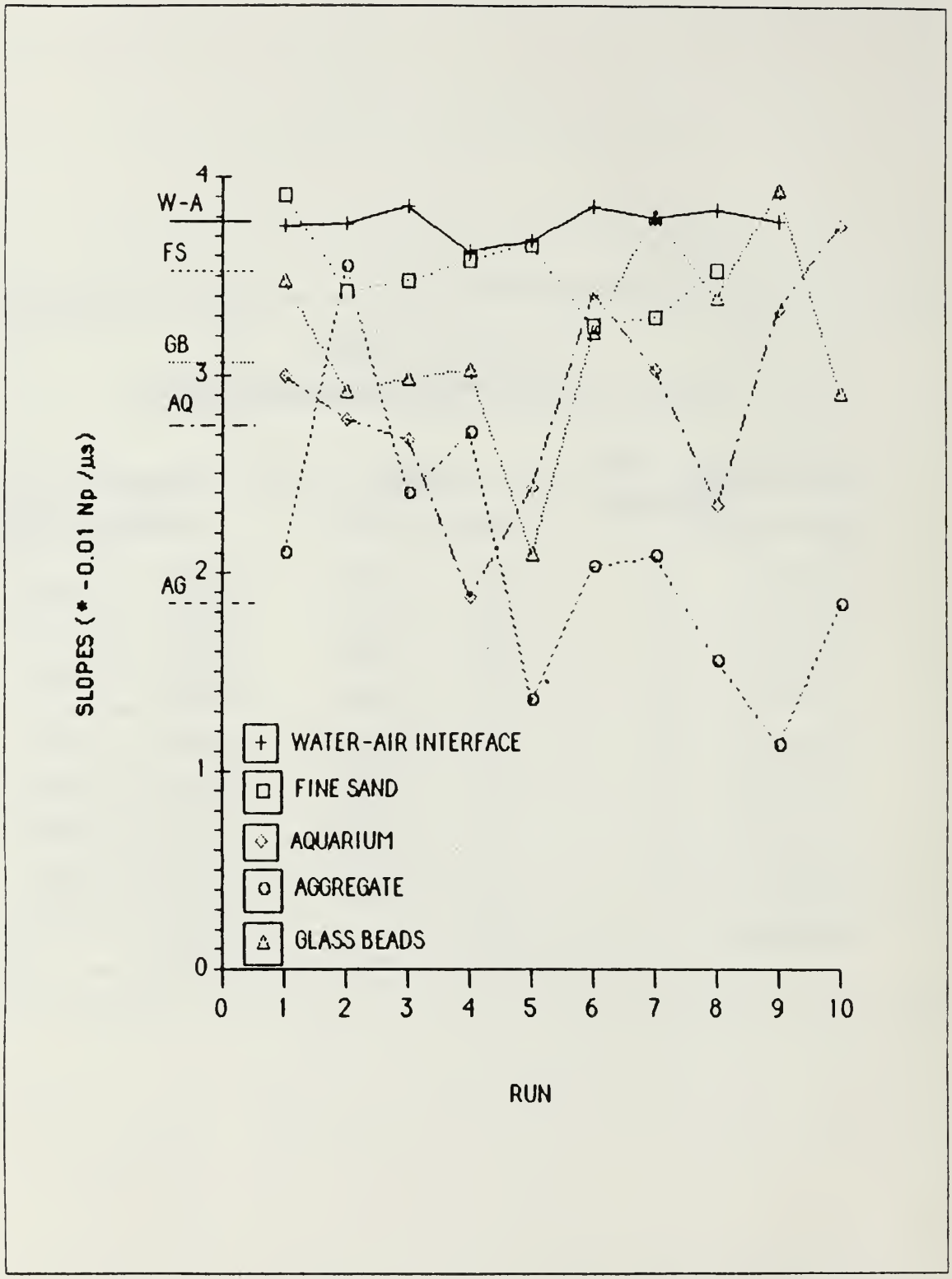

Figure 5.1 Spread of individual slopes.

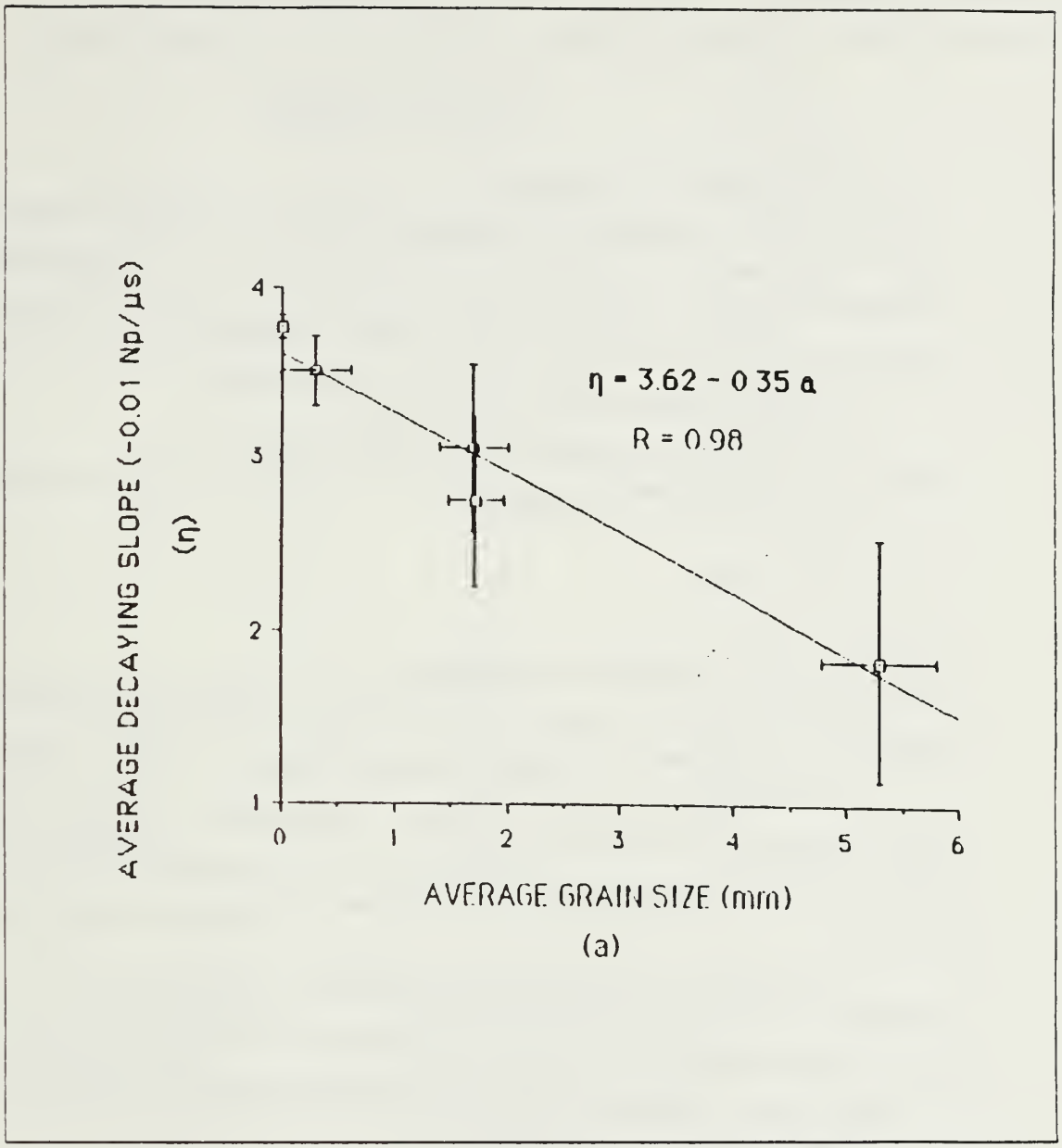

Figure 5.2 final averaged slopes vs grain size.

VI. CONCLUSIONS

The purpose of this experiment is to establish a relationship between acoustic volume scattering coefficients and sediment grain sizes. In the experimental design only volume reverberation was to be measured, and surface scattering was to be considered negligible. Surface scattering was not negligible for most of the materials studied, and it was not possible to achieve the initial purpose.

Nevertheless some conclusions can be drawn:

1. It was found that sediment grain size is related to the decay constant of the tail of the scattered pulse by the equation

$$a = 10.34 - \eta/0.35 \qquad (6.1)$$

This equation has, however, some limitations since it is applied to the decay constant of the specific transducer used and to the frequency of 180 kHz. It can be used, however, if the transducer is calibrated to a decay constant $\alpha = -3.77 \times 10^{-2}$ Np/μs.

2. For wavelengths of the same order of magnitude as the average grain size, surface scattering is an important component of the reverberation level, even if the sediment surface is perfectly levelled and smoothed, and depends also on the sediment's grain size.

3. The frequency used and materials selected for the experiment correspond to a wide range of ka values, from 0.12 for the *fine sand* to 4.16 for the *aggregate*. The decaying slope monotonically decreases with increasing grain size and does not show any strange behavior in the region of ka = 1.

4. Inhomogeneities in sediment composition are not responsible for the variation in the decaying slopes obtained, at least not totally, since measurements made on homogeneous material like *glass beads* show the same spread in results as the *aquarium sand* of similar size.

Further study of the volume reverberation from ocean sediments is recommended, as is the use of different combinations of frequency and grain sizes, keeping in mind that wavelengths of the same order of magnitude as the grain size should not be used so that surface scattering may be neglected.

A theoretical search must be done to investigate the influence of transducer characteristics on the decay constant, to verify the extent of the validity of Equation 6.1.

APPENDIX
DATA COLLECTING AND PROCESSING SEQUENCE

In this appendix a complete sequence of the data collecting and processing for the fine sand is presented. Eight data sets (DATA#) of 50 pulses each were collected for this sediment and averaged using the program THESIS3. These data sets (files DATA41 to 48) are graphically represented in Figures 1 to 8 where the squared voltages are plotted against time (program PLOT).

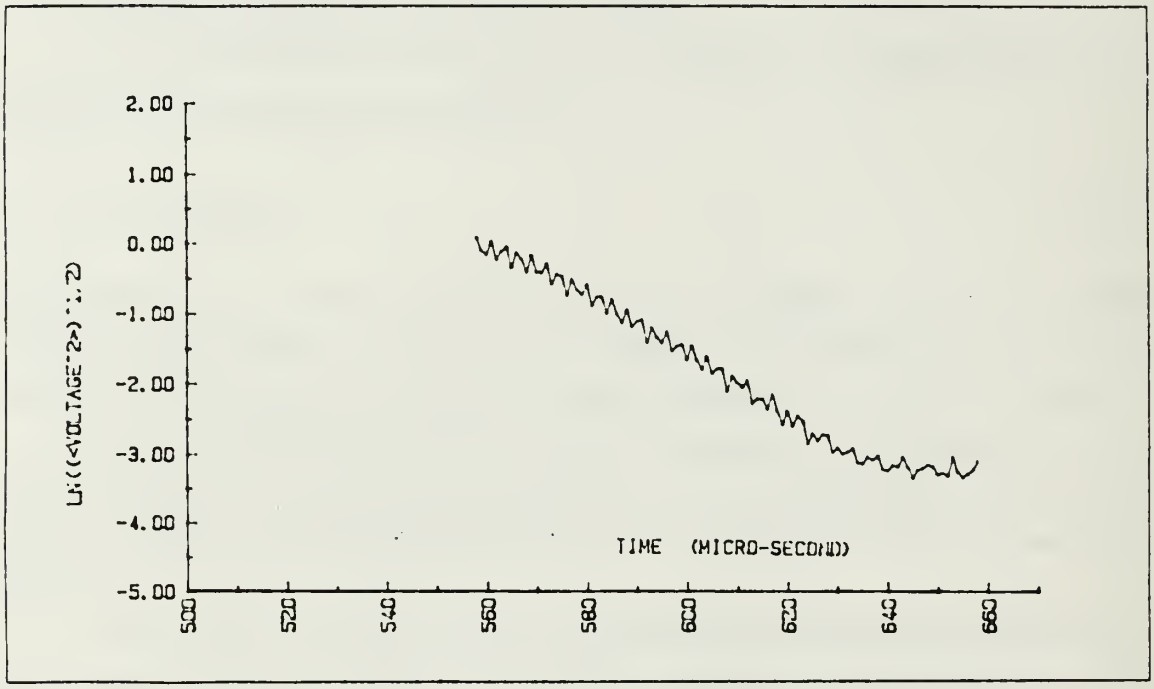

Figure 1 Pulse waveform of DATA41.

The decaying slopes for these pulses are then determined using the program MAXIMUM that selects the points of local maximum voltages. A list of these points on the pulse tail for the first data set (DATA41)is presented next.

LISTING OF LOCAL MAXIMA FOR DATA41

		TIME (SEC.)	VOLT
J=	0	.000558	1.07504419
J=	1	.000561	1.01736522
J=	2	.000564	.93823038
J=	3	.000566	.86611777
J=	4	.000569	.80323466
J=	5	.000572	.74248771
J=	6	.000574	.69677940
J=	7	.000577	.59639584
J=	8	.000580	.55201449
J=	9	.000583	.46488708
J=	10	.000585	.44724043
J=	11	.000588	.38623309
J=	12	.000591	.33518950
J=	13	.000593	.29741553
J=	14	.000596	.27842414
J=	15	.000599	.23419650
J=	16	.000601	.22929457
J=	17	.000604	.19638737
J=	18	.000606	.16494848
J=	19	.000609	.14870104
J=	20	.000612	.14002857
J=	21	.000615	.10873822
J=	22	.000617	.11429786
J=	23	.000620	.09046546
J=	24	.000622	.08471127
J=	25	.000625	.06627217
J=	26	.000627	.06566582
J=	27	.000630	.05425864
J=	28	.000633	.05396295
J=	29	.000636	.04774935
J=	30	.000638	.04841487
J=	31	.000641	.04233202
J=	32	.000643	.04783304
J=	33	.000648	.04280187
J=	34	.000651	.03784178
J=	35	.000653	.04774935

The corresponding waveform envelope is plotted in Figure 9. It is obtained by connecting the points of maximum voltage. The best fitted straight line and corresponding slope are then determined (program PLOT3).

The individual slopes show big spread (see Chapter five), and they were applied in the averaging process. The eight data sets were averaged as follows:

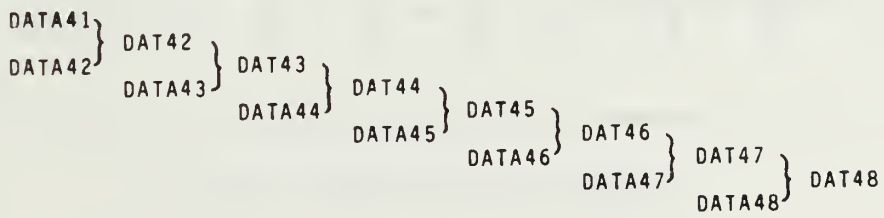

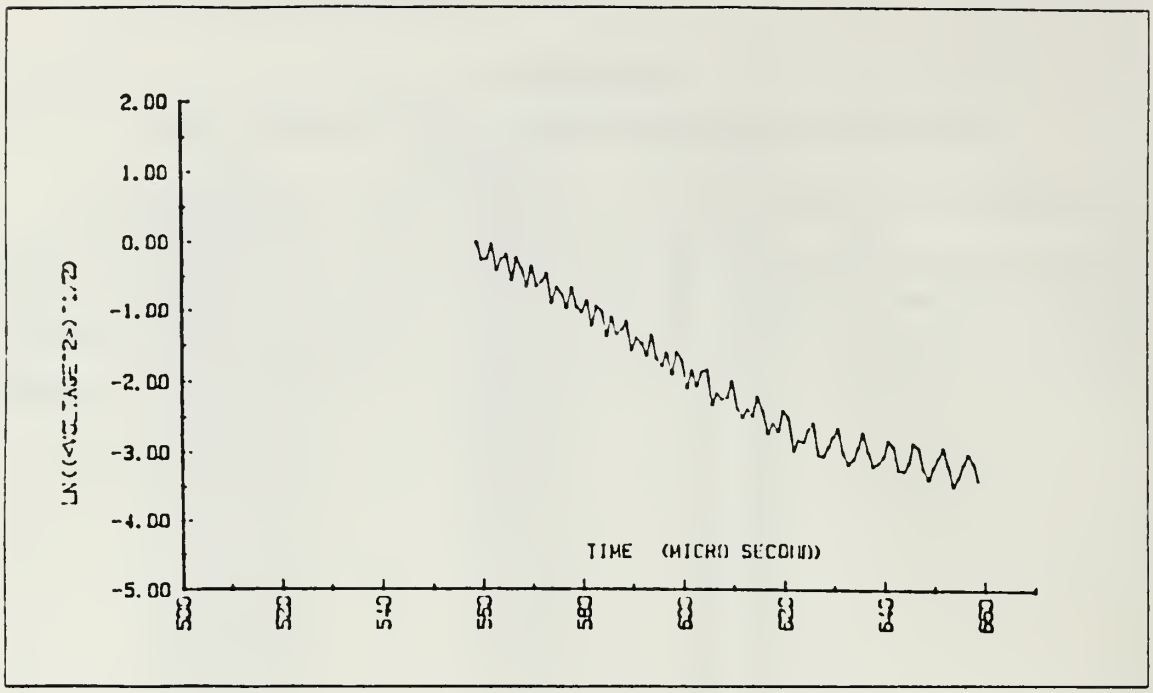

Figure 2 Pulse waveform of DATA42.

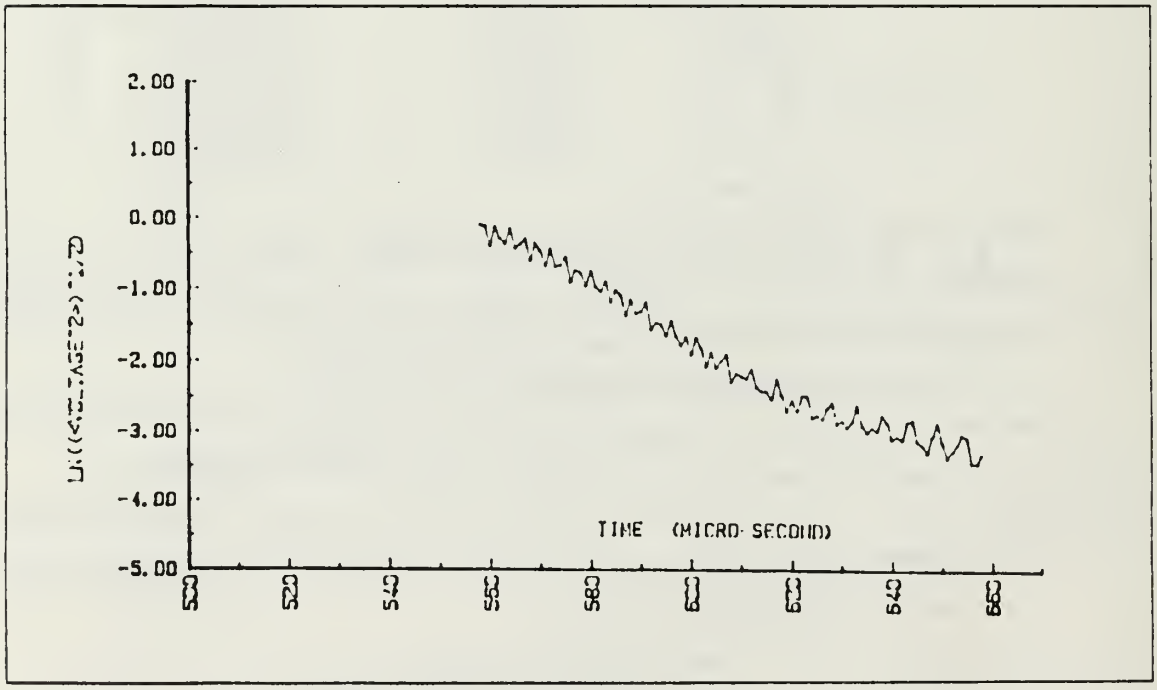

Figure 3 Pulse waveform of DATA43.

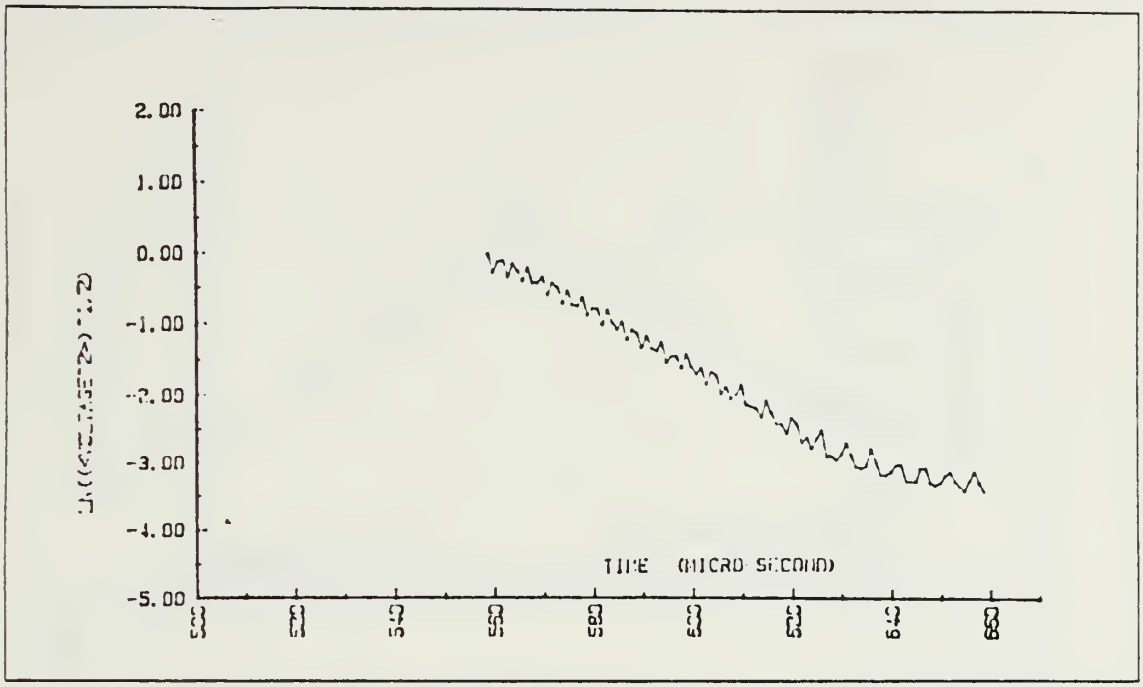

Figure 4 Pulse waveform of DATA44.

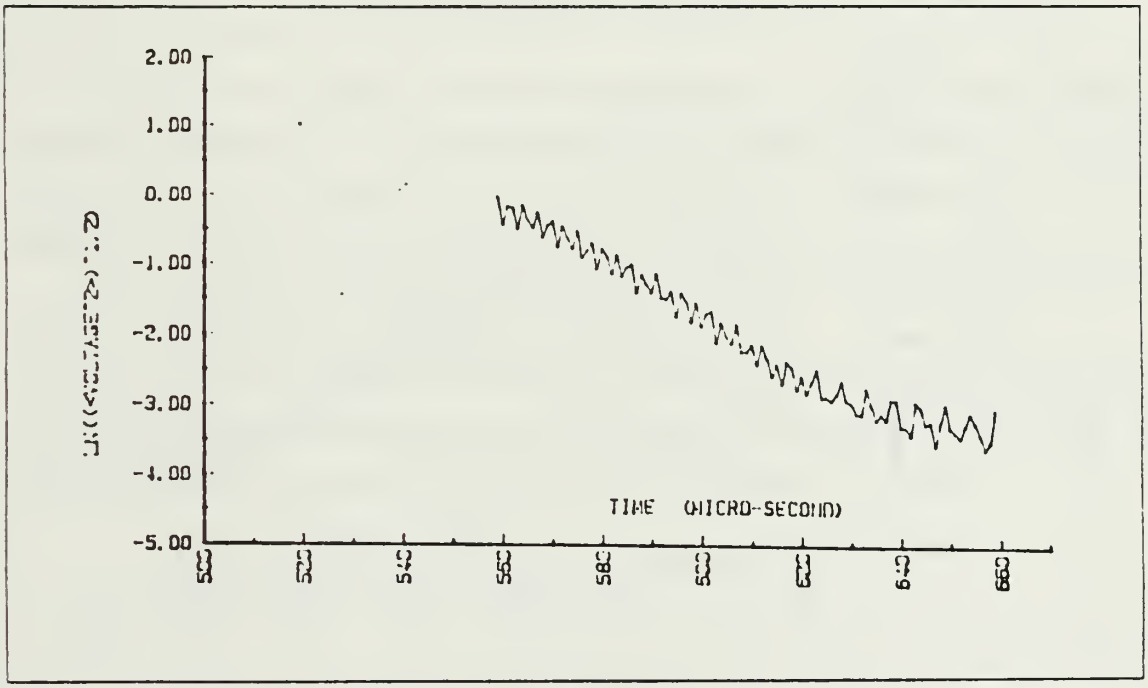

Figure 5 Pulse waveform of DATA45.

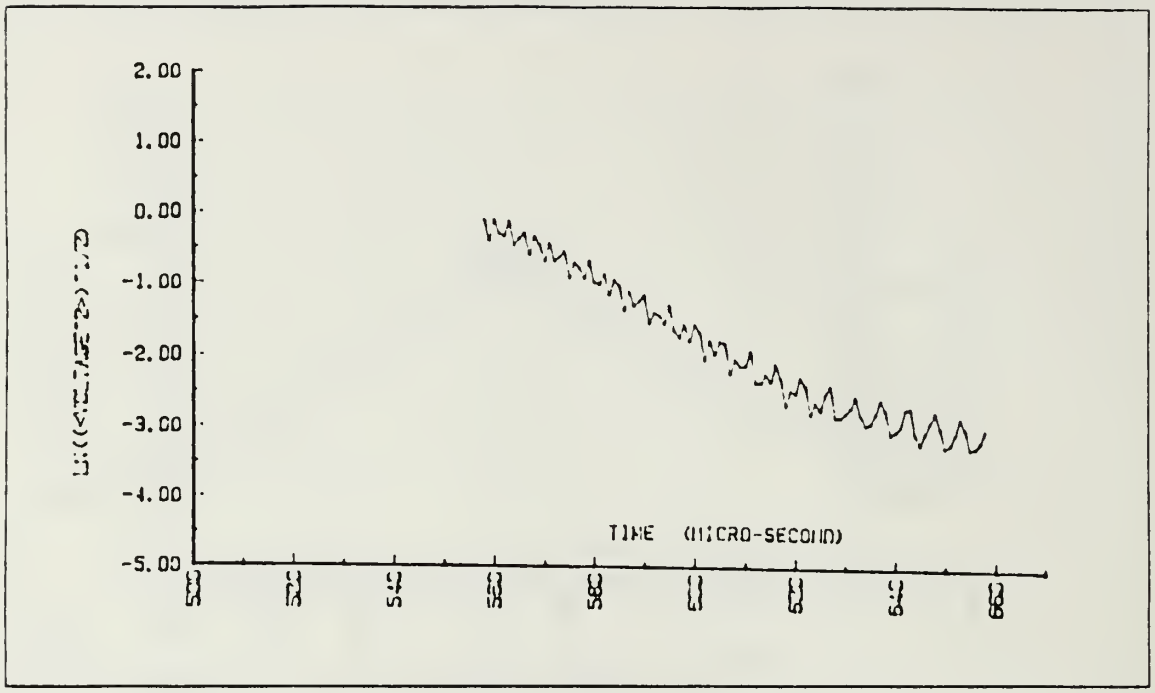

Figure 6 Pulse waveform of DATA46.

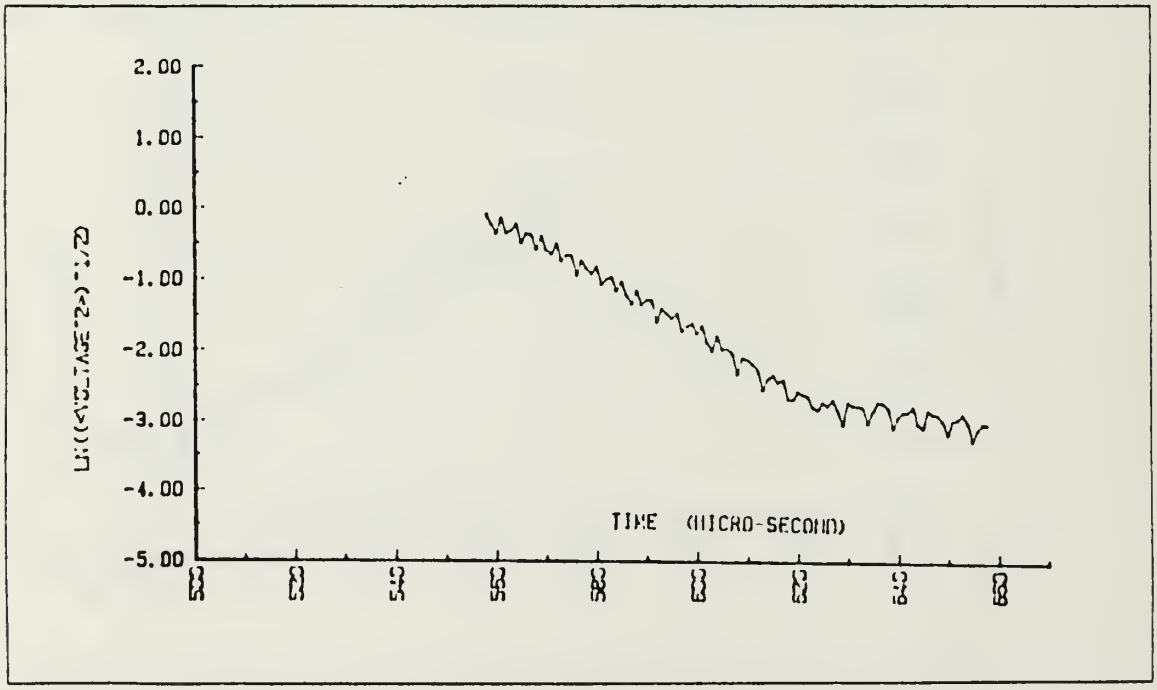

Figure 7 Pulse waveform of DATA47.

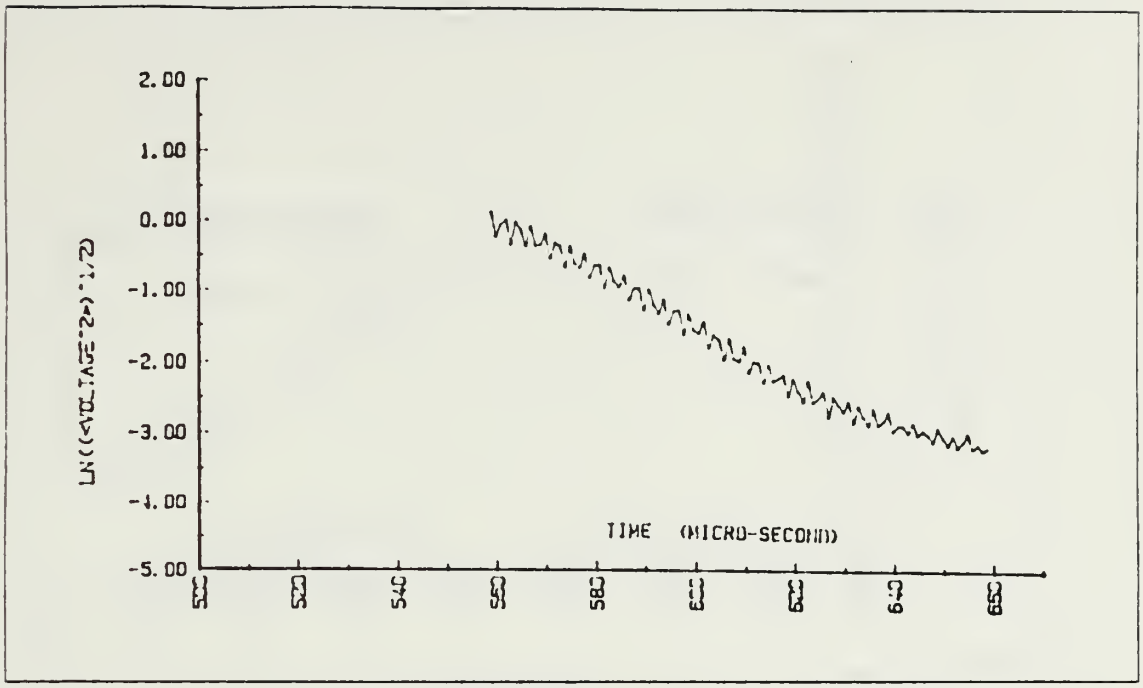

Figure 8 Pulse waveform of DATA48.

DAT42 is the average of DATA41 and DATA42. From DAT42 to DAT48 the variations presented in the individual waveforms are filtered because the number of terms involved in the average increases. DAT48, the result of the averaging, may be considered the representative waveform for the fine sand.

Next, programs MAXIMUM and PLOT3 are applied to the averaged DAT# sets which corresponding plots are presented in Figures 10 to 17.

The envelope from DATA41 to DAT48 gets smoother and the value of the decaying slope stabilizes along the averaging process although the differences are small since the individual waveforms are not very different for this sediment.

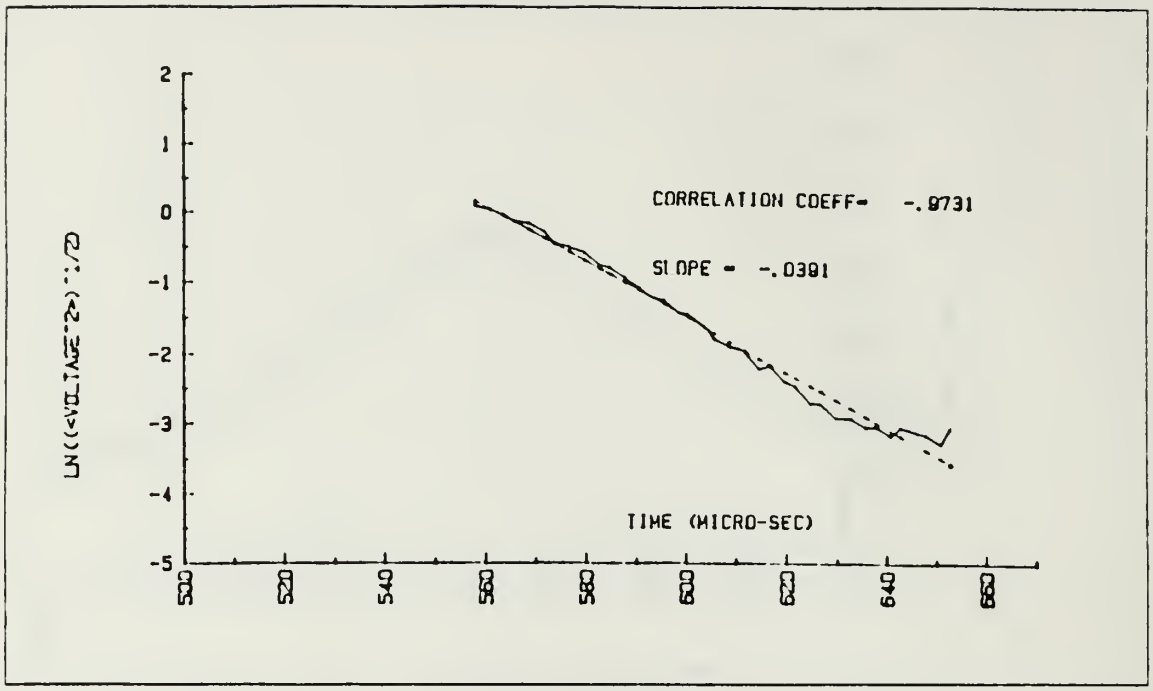

Figure 9 DATA41.

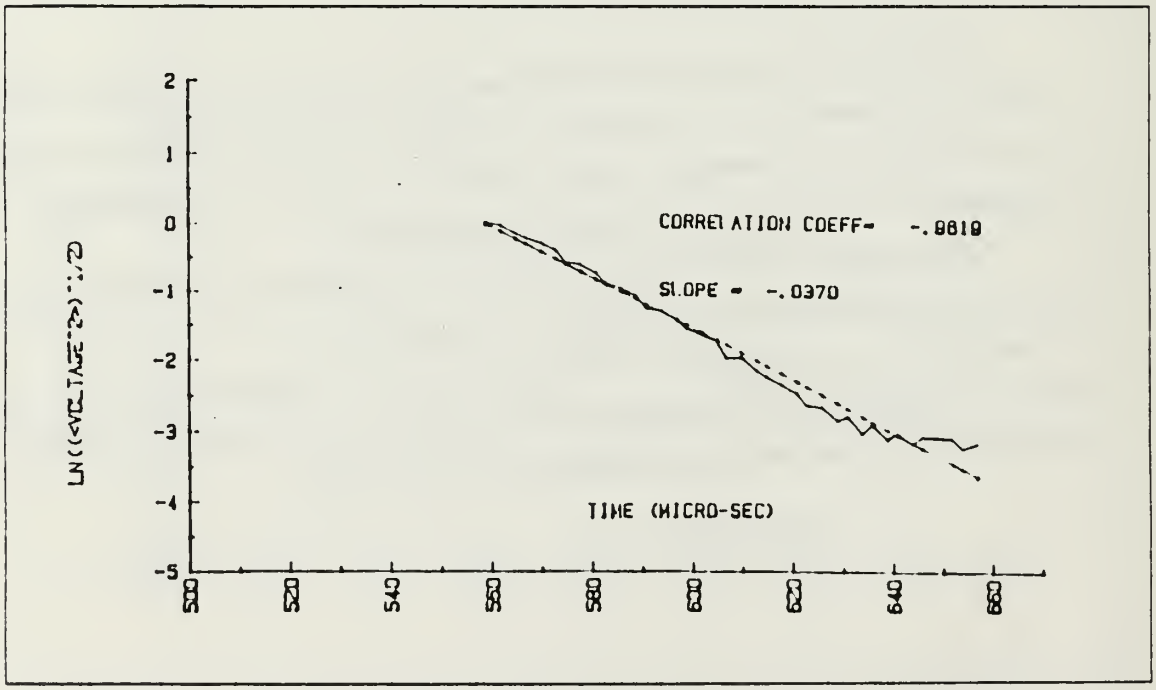

Figure 10 DAT42.

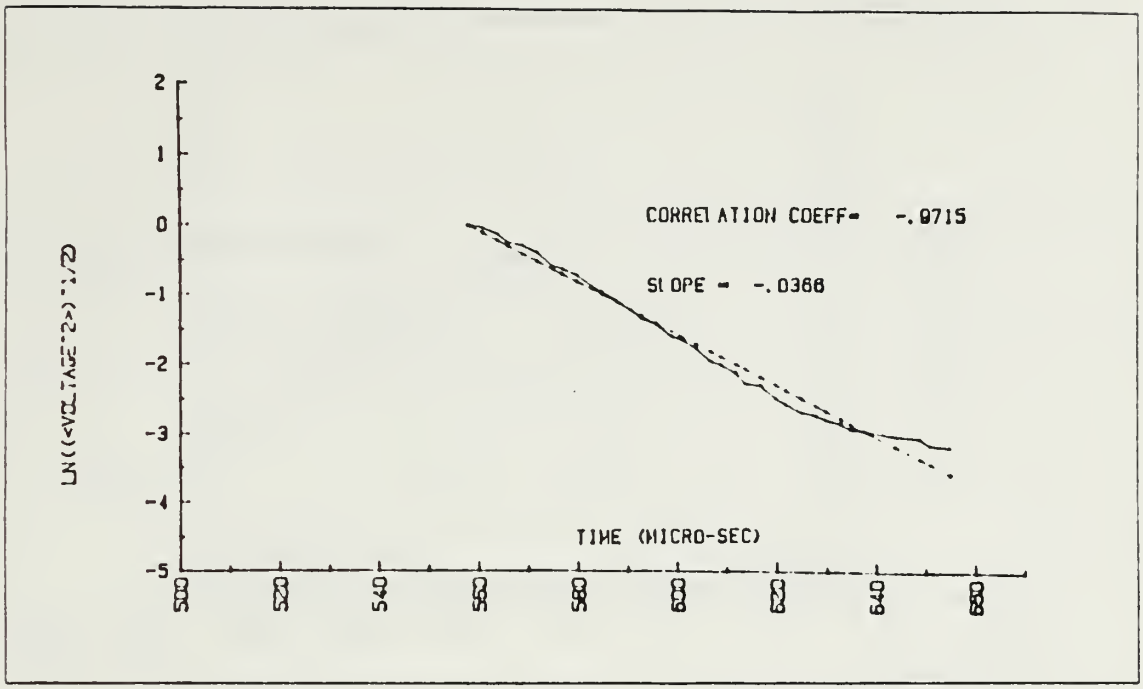

Figure 11 DAT43.

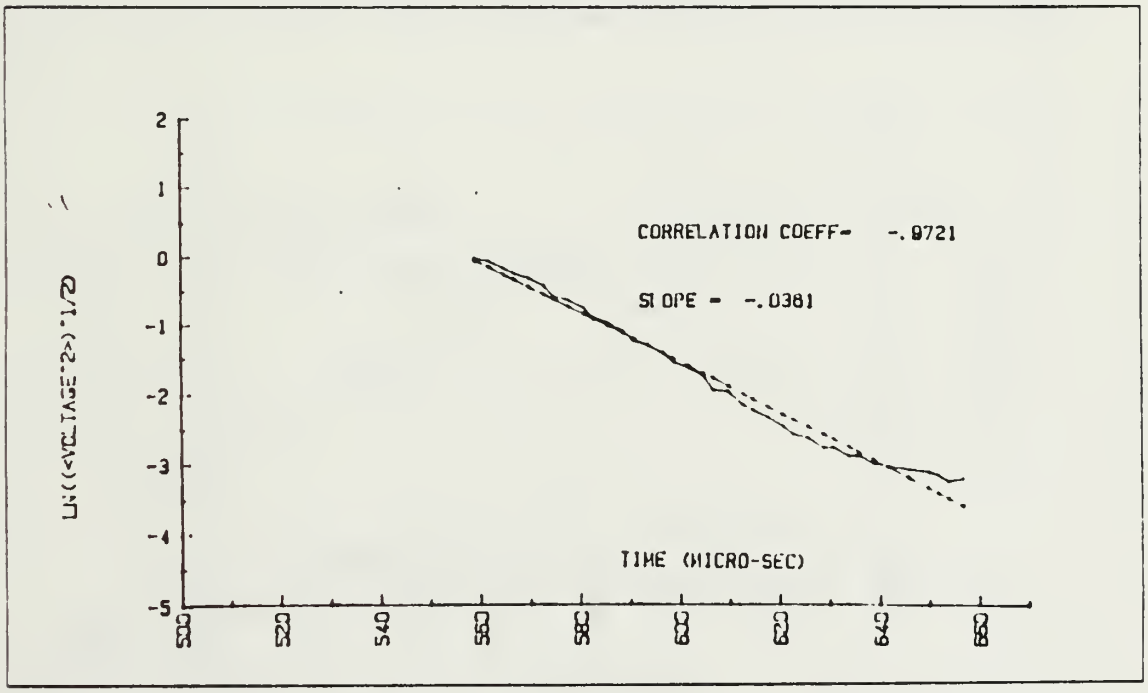

Figure 12 DAT44.

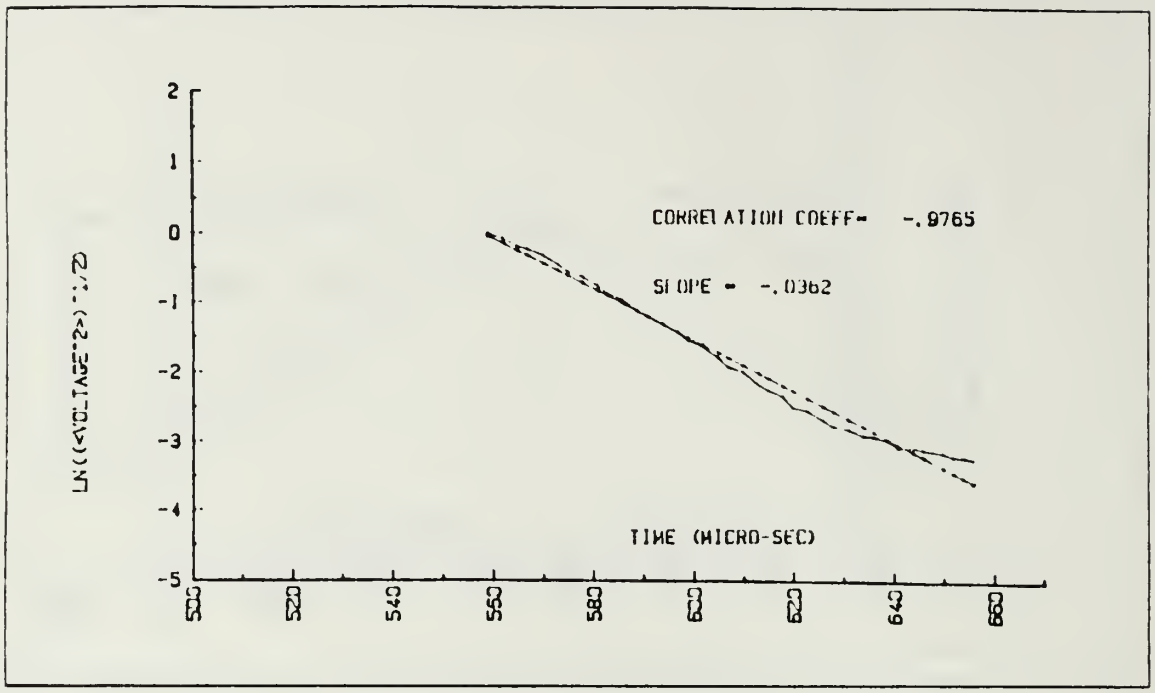

Figure 13 DAT45.

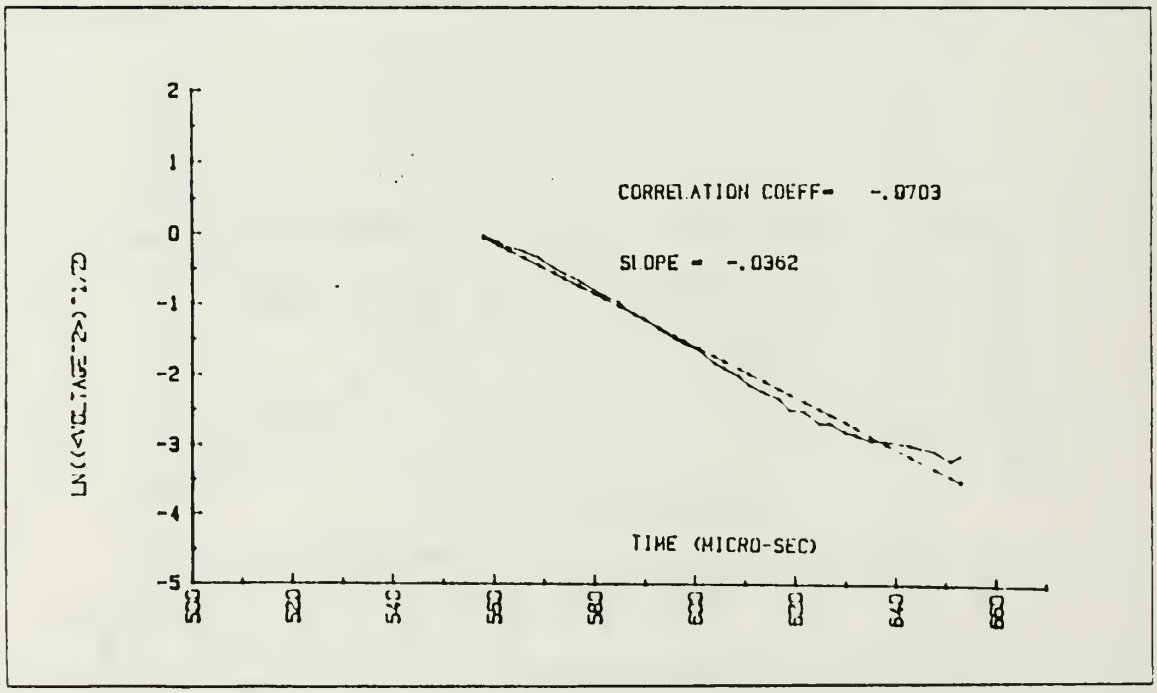

Figure 14 DAT46.

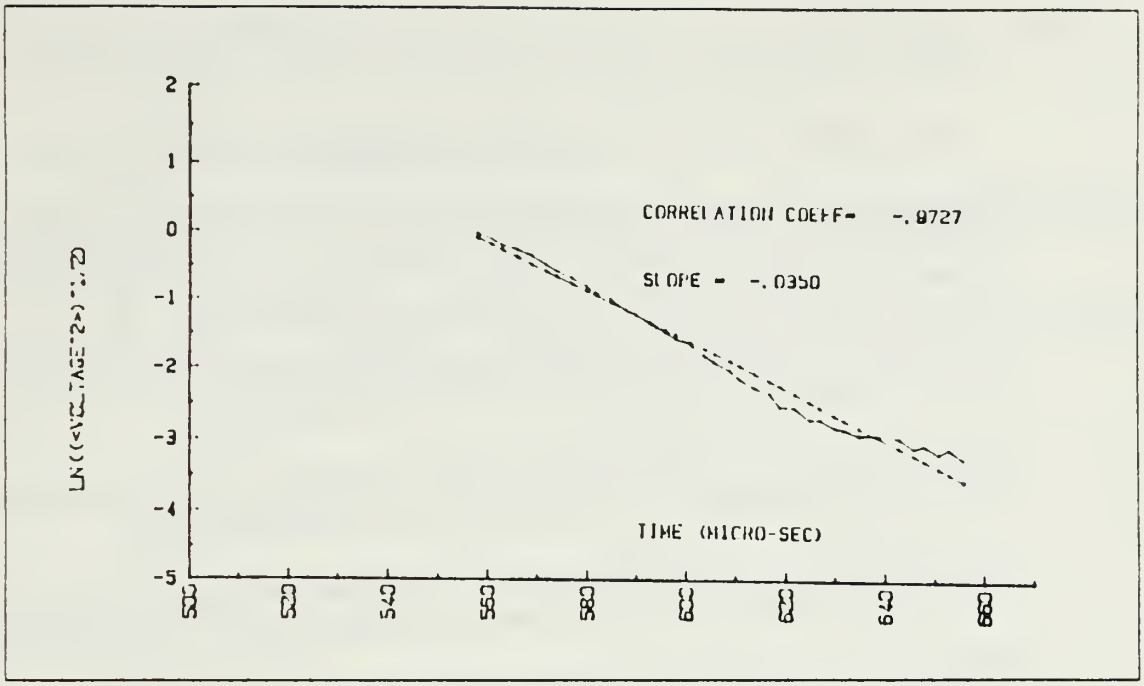

Figure 15 DAT47.

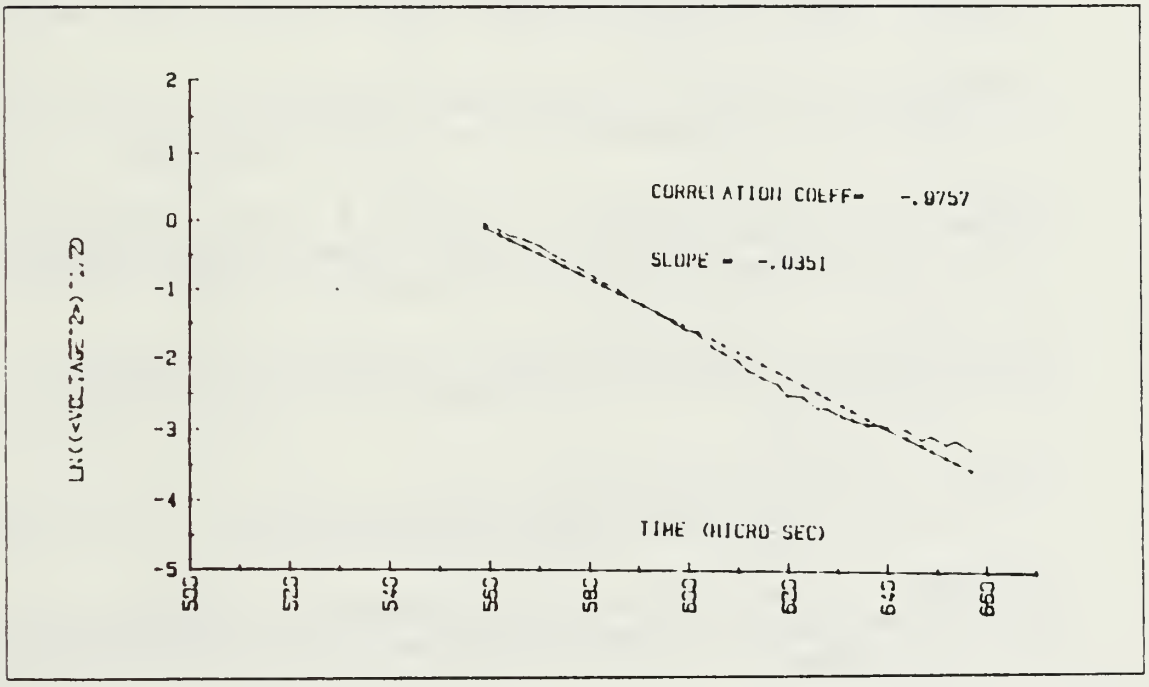

Figure 17 DAT48.

LIST OF REFERENCES

Hamilton, E.L., Shumway, G., Menard, H. W. and Shipek C. J., Acoustic and other Physical Properties of Shellow - Water Sediments off San Diego. *The Journal of Acoustical Society of America*, Volume 28, No. 1, January 1956.

Urick, R. J., The Backscattering of Sound from a Harbor Bottom. *The Journal of Acoustical Society of America*, Volume 26, No. 2, March 1954.

Chang. Chin-Wen., *Remote Sensing of Ocean Sediment Volume Reverberation*, M. S. Thesis, Naval Postgraduate School, Monterey, CA., December 1986.

Mackenzie, K. V., Bottom Reverberation for 530 and 1030 cps Sound in Deep Water, *The Journal of Acoustical Society of America*, Volume 33, No. 11, November 1961.

Dodds, D. J., Surface and Volume backscattering of broadbard acoustic pulses normally incident on the seafloor: Observation and Models, *The Journal of Acoustical society of America*, Suppl. 1, April 1984.

Meng, J., Guan, D., Acoustical method for remote sensing of seafloor sediment types, *Acta Acust. (China)*, Volume 7, No. 6, Nov. 1982.

Bradshaw, J. A., *Laboratory Study of Sound Propagation into a Fast Bottom Medium*, M. S. Thesis, Naval Postgraduate School, Monterey, CA., June 1981.

Clarke, T. L., Proni, J.R., Seem, D. A., and Tsai, J. J., *Joint CGS-AOML Acoustical Bottom Echo-Formation Research I: Literature Search and Initial Modeling Results*, NOAA Technical Memorandum ERL-AOML, Miami, FL., 1984.

Diaz, Frederico R., *Preliminary Study of a Technique for Measuring the Volume Backscattering from Sediments*, M. S. Thesis, Naval Postgraduate School, Monterey, CA., September 1986.

Kinser, L. E., Frey, A. R., Coppens, A. B. and Sanders, J. V., *Fundamentals of Acoustics*, Third Edition, Wiley & Sons, Inc.,New York, 1982.

McKinney, C. M. and Anderson, C. D., Measurements of Backscattering of sound from the Ocean Bottom. *The Journal of The Acoustical Society of America*, Volume 36, No. 7, January 1964.

Morse P. M. and Ingard, K. U., *Theoretical Acoustics* First Edition, McGraw-Hill, Inc., 1968.

National Defense Research Commitee, *Physics of Sound in the Ocean*, Headquarters Naval Material Command, Department of Navy,Washington D.C. 1969.

Nicholet Instrument Corporation, *Nicholet 3091 Operating Manual*, 1985

Urick, U. J., *Principles of Underwater Sound*, Third Edition, McGraw-Hill, Washington D. C., 1983.

Urick, R. J., *Sound Propagation in the Sea*, Defense Advanced Research Projects Agency (DARPA), Washington D. C.,1979.

INITIAL DISTRIBUTION LIST

		No. Copies
1.	Defense Technical Information Center Cameron Station Alexandria, VA 22304-6145	2
2.	Library, Code 0142 Naval Postgraduate School Monterey, CA 93943-5002	2
3.	Chairman, Department of Oceanography Code 68 Naval Postgraduate School Monterey, CA 93943	1
4.	Cherry, James R. Code 68CH Naval Postgraduate School Monterey, CA 93943	1
5.	Professor J. V. Sanders, Code 61Sd Department of Physics Naval Postgraduate School Monterey, CA 93943	2
6.	Professor A. B. Coppens, Code 61Cz Department of Physics Naval Postgraduate School Monterey, CA 93943	1
7.	Professor S. P. Tucker, Code 68Tx Department of Oceanography Naval Postgraduate School Monterey, CA 93943	2
8.	Director, Charting and Geodetic Sciences N/CG, Room 1006, WSC-1 National Oceanic and Atmospheric Administration Rockville, MD 20552	1
9.	Facada, Joao Instituto Hidrografico Rua das Trinas 49 1296 Lisboa Codex PORTUGAL	5

10. John R. Proni
National Oceanic and Atmospheric Administration
Atlantic Oceanographic and Meteorological Laboratory 1

11. Yu, Ta-Te
SMC#1343 Naval Postgraduate School 1
Monterey, CA 93943

12. Professor Von Schwind, Code 68Vs
Department of Oceanography 1
Naval Postgraduate School
Monterey, CA 93943

13. Wang, Chin-Ping 1
SMC # 1342 Naval Postgraduate School
Monterey, CA 93943

14. Chang, Ching-Wen 1
PO Box 8505
Tso-Ying, kaohsung, Taiwan
Republic of China

Thesis
F147 Facada
c.1 Volume reverberation
measurements of sediments
in the laboratory.